The Geological Society of America
Special Paper 511
2015

Petrology, geochemistry, and ages of lavas from Northwest Hawaiian Ridge volcanoes

Michael O. Garcia
Department of Geology and Geophysics, SOEST, University of Hawai'i at Mānoa, Honolulu, Hawai'i 96822, USA

John R. Smith
Hawai'i Undersea Research Laboratory, SOEST, University of Hawai'i at Mānoa, Honolulu, Hawai'i 96822, USA

Jonathan P. Tree
Department of Geology and Geophysics, SOEST, University of Hawai'i at Mānoa, Honolulu, Hawai'i 96822, USA

Dominique Weis
Lauren Harrison
Pacific Centre for Isotopic and Geochemical Research, Department of Earth, Ocean and Atmospheric Sciences, University of British Columbia, Vancouver, BC V6T1Z4, Canada

Brian R. Jicha
Department of Geoscience, University of Wisconsin-Madison, Madison, Wisconsin 53706, USA

ABSTRACT

The Northwest Hawaiian Ridge is a classic example of a large igneous province. The morphology and geology of the ridge is poorly characterized, although it constitutes the longest segment (~47%) of the Hawaiian-Emperor Chain. Here we present a new bathymetric compilation, petrographic and X-ray fluorescence (XRF) data for lavas from 12 volcanoes along the Northwest Hawaiian Ridge, and review literature data for the age and isotopic variation of the ridge. The bathymetric compilation revealed that the Northwest Hawaiian Ridge consists of at least 51 volcanoes. The 45 new XRF analyses show that the Northwest Hawaiian Ridge contains tholeiitic and alkalic lavas with compositions typical of lavas from the Hawaiian Islands. The absolute ages and duration of volcanism of individual Northwest Hawaiian Ridge volcanoes are poorly known, with modern $^{40}Ar/^{39}Ar$ ages for only 10 volcanoes, mostly near the bend in the chain. We infer the initiation age of the Hawaiian-Emperor Bend to be ca. 49–48 Ma, younger than the age for the onset of island arc volcanism in the western Pacific (52–51 Ma). Thus, the kink in the Hawaiian-Emperor Chain and the onset of arc volcanism were not synchronous. Isotopic data are sparse for the Northwest Hawaiian Ridge, especially for Pb and Hf. Two transitional lavas from just south of the bend have Loa trend type Pb and Sr isotopic ratios. Otherwise, the available chemistry for Northwest Hawaiian Ridge lavas indicates Kea-trend source compositions. The dramatic increase in melt flux along the Hawaiian Ridge (~300%) may be related to changes in melting conditions, source fertility, or plate stresses.

Garcia, M.O., Smith, J.R., Tree, J.P., Weis, D., Harrison, L., and Jicha, B.R., 2015, Petrology, geochemistry, and ages of lavas from Northwest Hawaiian Ridge volcanoes, *in* Neal, C.R., Sager, W.W., Sano, T., and Erba, E., eds., The Origin, Evolution, and Environmental Impact of Oceanic Large Igneous Provinces: Geological Society of America Special Paper 511, p. 1–25, doi:10.1130/2015.2511(01).

INTRODUCTION

The Hawaiian-Emperor Chain (Fig. 1) is the classic example of a hotspot chain formed by a mantle plume (e.g., Wilson, 1963; Morgan, 1971). It is one of the tectonically simplest (distant from any plate margin or continent for more than 70 m.y.) and longest examples of an oceanic island chain or hotspot track, with >100 volcanoes formed over 82 m.y. and extending ~6000 km in length (Fig. 1). The active southeast portion of the chain (the Hawaiian Islands) is surrounded by an ~1000-km-wide bathymetric swell, which is thought to be associated with a hot buoyant mantle plume beneath the lithosphere (e.g., Ribe and Christensen, 1999). Many studies have suggested that the classic view of mantle plumes is too simplistic (e.g., heat flow pattern not as predicted; Von Herzen et al., 1989; hotspots are not fixed; Tarduno et al., 2003, 2009). These and other complications led some to question the existence of mantle plumes, even for Hawai'i (Foulger and Jurdy, 2007). The discovery of a seismically defined deep conduit under the Island of Hawai'i (Wolfe et al., 2011), together with the association of enriched geochemical signatures in oceanic islands related to deep mantle sources (Weis et al., 2011; Huang et al., 2011), has renewed support for the deep mantle plume hypothesis.

Is the Hawaiian-Emperor Chain a large igneous province (LIP)? Coffin and Eldholm (1992, 1994) included the Hawaiian-Emperor Chain within the seamount group of LIPs. A revised LIP definition (Sheth, 2007) recommended a new subcategory, large basalt provinces, which eliminated many oceanic island and seamount groups but included the Hawaiian-Emperor Chain as an example along with classic continental examples (e.g., Deccan Traps Basalt and Columbia River Basalt). A more restricted definition by Bryan and Ernst (2008, p. 175) stated "Large Igneous Provinces are magmatic provinces with areal extents (>0.1 Mkm^2), igneous volumes (>0.1 Mkm^3) and maximum lifespans of ~50 m.y. that have intraplate tectonic settings or geochemical affinities, and are characterised by igneous pulses of short duration (~1–5 m.y.), during which a large proportion (>75%) of the total igneous volume has been emplaced." The Hawaiian-Emperor Chain qualifies in tectonic setting, area, and volume (~6 Mkm^3) but not in duration of formation (it is too long, >80 m.y.). However, if only the Hawaiian Ridge portion of the chain is considered, it qualifies as an LIP using the new definition because its activity covers <50 m.y. and each shield volcano probably formed over a period of <5 m.y. (Sharp and Clague, 2006; Garcia et al., 2006). Regardless of the definition used, the Hawaiian-Emperor Chain has been recognized as a major basaltic province for more than 100 years (Dana, 1890). We show here that much of Hawaiian Ridge is poorly known and deserves better geological, geochemical, and geochronological characterization.

The purpose of this paper is to provide an update on the current knowledge of the age and isotopic variations along the Northwest Hawaiian Ridge, the part of the ridge northwest of the Hawaiian Islands (Fig. 1). We also provide new petrographic and XRF data for lavas recently collected using the University of Hawai'i's HOV (Human Occupied Vehicle) submersible *Pisces V*, as well as dredged and island samples from the University of Hawai'i and Scripps Institution of Oceanography rock collections for 12 volcanoes. The submersible dives were part of a reconnaissance survey of the new U.S. marine sanctuary, Papahānaumokuākea Marine National Monument. Our sample suite extends from Nīhoa (in the southeast) to Academician Berg Seamount (in the northwest), spanning ~1900 km of the ridge (Fig. 1) and across the entire monument. Many critical questions remain unresolved about the Northwest Hawaiian Ridge, including the age progression of volcanoes (e.g., several volcanoes over a 1000 km section have reported ages of ca. 27 Ma), mantle source (whether both the Kea and Loa source compositions or other components are present), and the cause of the dramatic (300%) increase in its melt flux (Vidal and Bonneville, 2004) for the Hawaiian Ridge. New age and other geochemical data will have fundamental implications for the Hawaiian mantle plume source components and dynamics, and for our understanding of Cenozoic plate kinematics. This paper highlights the gaps in our knowledge base for age and composition of lavas from the Northwest Hawaiian Ridge.

GEOLOGIC BACKGROUND

The Hawaiian-Emperor Chain can be subdivided into three segments (Fig. 1) from north to south: Emperor Seamounts (north of the bend, ~2500-km-long segment with at least 45 volcanoes; Clague, 1996), Northwest Hawaiian Ridge (south of the bend to Middle Bank Seamount, ~2800-km-long segment with at least 51 volcanoes; see below for the criteria used here), and the Hawaiian Islands (Ni'ihau to the Island of Hawai'i, ~700 km long with at least 19 volcanoes). The geochemistry and ages of lavas from the Hawaiian Islands have been and continue to be intensively investigated (e.g., Sherrod et al., 2007; Garcia et al., 2010; Weis et al., 2011, and references therein). In contrast, the other two segments of the Hawaiian-Emperor Chain have received only piecemeal sampling and study. The Emperor Seamounts have been better sampled than the Northwest Hawaiian Ridge as a result of four Ocean Drilling Program Legs (19, 55, 145, and 197; e.g., Jackson et al., 1980; Duncan et al., 2006) and several dredging expeditions (see Clague and Dalrymple, 1987). These studies created a good characterization of the age and geochemistry of the lavas from many of the seamounts using modern high-precision methods (e.g., Regelous et al., 2003; Duncan and Keller, 2004; Huang et al., 2005; Sharp and Clague, 2006). These studies also showed that the Emperor Seamounts formed from the same mantle source, and had multistage growth histories similar to those of Hawaiian Island volcanoes. The variations in geochemistry and isotopic compositions of shield lavas along the Emperor Seamounts have been explained by a thickening lithosphere over the hotspot, which controlled the depth and extent of partial melting (e.g., Regelous et al., 2003; Huang et al., 2005).

The Northwest Hawaiian Ridge (south of the bend to the northern Hawaiian Island of Ni'ihau; Fig. 1) was sampled spo-

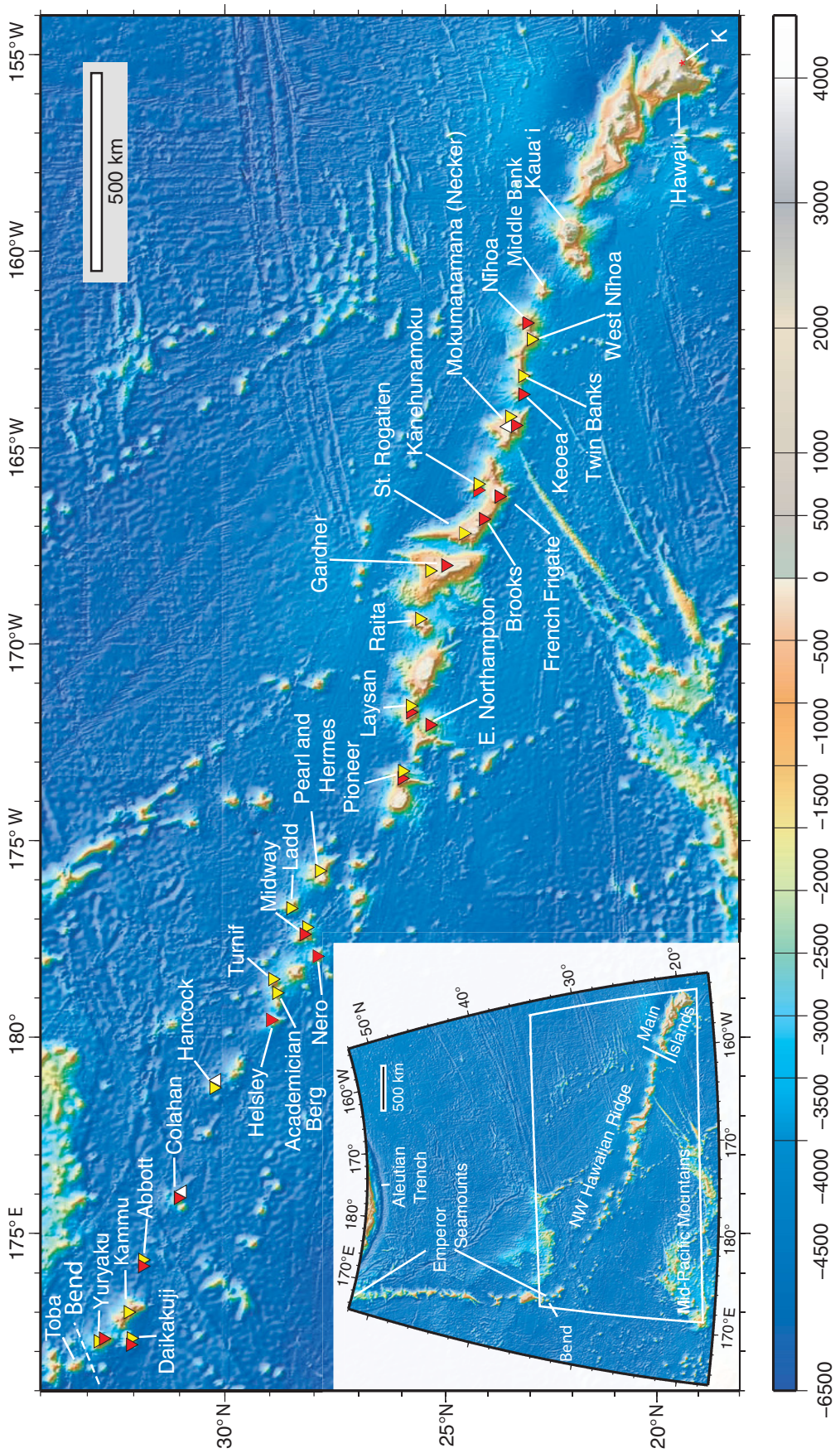

Figure 1. Map of the Northwest Hawaiian Ridge based on the SRTM30_PLUS (Shuttle Radar Topography Mission) bathymetry data set (Becker et al., 2009). Red triangles show locations where shield stage lavas (tholeiites) have been recovered; yellow triangles show where post-shield stage transitional and alkalic lavas have sampled; white triangles show where rejuvenation-stage rocks were obtained. Note that many Northwest Hawaiian Ridge volcanoes have no geochemical data. The location of the Kīlauea reference point at the center of its summit caldera is shown by the K at 155.273840°W, 19.413017°N. This point was used for making the distance estimates given in Table 1. The data were gridded at 1 km spacing (~30 arc s). A Mercator projection was used for map. Inset: Map of the north-central Pacific Basin showing the Hawaiian-Emperor Chain, Mid-Pacific Mountains and Aleutian Trench. A transverse Mercator projection was used (white box shows location of main map).

radically in several dredging programs in the 1970s and 1980s, and in 1999 in the northern part of the ridge. Midway Atoll was drilled in 1963–1964 (two holes, 173 and 504 m deep) that recovered mostly carbonate rock but bottomed in basalt (Ladd et al., 1970). In addition, four islands (Necker, now called Mokumanamana, Nīhoa, French Frigate, and Midway) that represent remnants of shield volcanoes were sampled in 1968 (Dalrymple et al., 1974). Some of the recovered lavas were geochemically characterized (mostly for major elements) and dated using K-Ar methods (Clague and Dalrymple, 1987; Garcia et al., 1987). Lavas from two seamounts (Northampton and Laysan) were dated using ^{40}Ar-^{39}Ar methods, and analyzed by XRF for major and trace elements (Dalrymple et al., 1981). New ^{40}Ar-^{39}Ar ages and whole-rock major and trace element data for eight seamounts between the bend and Pearl and Hermes Seamount were presented by O'Connor et al. (2013). Lavas from Mokumanamana and Nīhoa islands and French Frigate, Gardner, and Northampton seamounts were studied for Nd and Sr isotopes (Basu and Faggart, 1996). Thus, this 2800-km-long portion of the Hawaiian chain (especially from Middle Bank to Midway) is poorly characterized geochemically and geochronologically, especially using modern methods. The current databases for age and isotope geochemistry of the Hawaiian Ridge are detailed below. Most of the Northwest Hawaiian Ridge is now part of the Papahānaumokuākea Marine National Monument, which is effectively closed to new lava sampling by dredging methods.

Most Hawaiian Island volcanoes follow an evolutionary sequence that is well documented (Macdonald et al., 1983; Walker, 1990), although the details continue to be refined (e.g., Sherrod et al., 2007; Garcia et al., 2010). The earliest lavas of each volcano formed either on the deep (~5 km) Cretaceous oceanic crust or on the flanks of an adjacent, earlier formed volcano. The Northwest Hawaiian Ridge volcanoes are generally much less voluminous than those from the Hawaiian Islands (except Gardner; Bargar and Jackson, 1974). Thus, most of these volcanoes formed as isolated features on the deep ocean floor (e.g., Midway; Fig. 1). However, some formed on the flanks of adjacent volcanoes similar to the Hawaiian Islands (e.g., Mokumanamana and Southeast Necker; Fig. 1). The typical eruptive sequence for Hawaiian volcanoes starts with pre-shield alkalic lavas (<1% of total volcano volume; Moore et al., 1982; Garcia et al., 2006), followed by voluminous tholeiitic lavas of the shield stage (95%–99% of volcano) capped by weakly alkalic lavas of the post-shield stage (1%–3%; Macdonald et al., 1983). Lavas formed during the pre-shield stage are deeply buried by subsequent volcanism (>3 km) and are unlikely to be sampled after shield stage volcanism. Post-shield stage lavas usually form a thin cap (e.g., <10 to ~1000 m on Mauna Kea volcano; Wolfe et al., 1997) on the upper parts of the subaerial shield volcanoes extending to near sea level. The entire eruptive sequence for Hawaiian shield volcanoes may take ~1.5 m.y. (Garcia et al., 2006). After a hiatus in eruptive activity of 0.5–2 m.y., new eruptions (rejuvenation stage; Ozawa et al., 2005) of strongly to moderately alkalic lavas occur on ~50% of the volcanoes within the Hawaiian Islands (Sherrod et al., 2007).

Assigning volcanic stage classifications to lavas collected by dredging and submersible from the Northwest Hawaiian Ridge is challenging in the absence of field relationships. Here we have used classifications based on petrography, and plots of the total alkalies versus silica (TAS) (Macdonald et al., 1983; Le Maître, 2002) and Nb/Y versus Zr/Y (Fitton, 2007). Rocks that plot below the Macdonald-Katsura line on the TAS diagram are tholeiitic and are considered to be from the shield stage. Alkalic lavas, which plot above the Macdonald-Katsura line, could be from the post-shield or rejuvenation stages. Only the post-shield stage has evolved alkalic rocks (Macdonald et al., 1983). Thus, alkalic rocks with silica >50 wt% (mugearites to trachytes) are likely to be from the post-shield stage. The Nb/Y versus Zr/Y plot appears to discriminate between alkalic basalts of the post-shield and rejuvenation stages. Rejuvenated rocks have higher Nb/Y ratios than those from the post-shield stage (Greene et al., 2010). These elements (Nb, Zr, and Y) are relatively insensitive to alteration, which is desirable for the Northwest Hawaiian Ridge rocks because they have undergone variable amounts of alteration. Where geochronologic data are available, ages are also used to evaluate volcanic stage relationships.

Subsidence on Hawaiian volcanoes occurs during and after their formation. It is initially rapid (2.6 mm/yr for the Island of Hawai'i) and thought to be related to loading of the lithosphere from the accumulation of lavas above the Hawaiian hotspot (e.g., Ludwig et al., 1991; Bianco et al., 2005). Later subsidence is slower and considered to be a consequence of lithospheric cooling (Phipps Morgan et al., 1995). Total subsidence varies (as inferred from a sharp slope change that marks the former shoreline that represents the maximum extent of the volcano as an island; e.g., Mark and Moore, 1987) with the age and size of the volcano (e.g., ~800 m for Middle Bank, a small isolated volcano at the southern end of the Northwest Hawaiian Ridge, versus ~2000 m for Gardner Seamount, a giant volcano near the center of the Northwest Hawaiian Ridge; Fig. 1). Coral reefs begin forming as the volcano approaches sea level and continue to grow as the volcano drifts off the hotspot to the northwest. The best-documented case within the Northwest Hawaiian Ridge is Midway volcano; drilling showed it is capped by ~400 m of coralline debris with some interbedded clay (Ladd et al., 1970). Thus, attempts to sample lavas from the northwest Hawaiian volcanoes must focus on their flanks to avoid carbonate rocks. Sampling at shallower depths (but below the carbonate platform) is likely to return lavas from the post-shield stage, whereas at deeper depths (>2000 m) the lavas are more likely to be tholeiitic. Rejuvenated rocks may form anywhere on the volcano, as seen for the northern Hawaiian Islands (e.g., Garcia et al., 2008).

NORTHWEST HAWAIIAN RIDGE VOLCANO INVENTORY

Here we present a new compilation of bathymetric data (Fig. 1), and a reevaluation of the number and location of volcanoes within the Northwest Hawaiian Ridge (Table 1). We have

TABLE 1. INVENTORY OF NORTHWEST HAWAIIAN RIDGE VOLCANOES BASED ON NEW BATHYMETRY

#	Volcano name	Distance from Kīlauea (km)	Long (°W)	Lat (°N)	Depth (mbsl)	Multi-beam	Age				XRF	Stage	Reference
							K-Ar	±2σ	Ar-Ar	±2σ			
1	Yuryaku	3541	172.28109	32.66244	615	P	31.0	1.0	47.4	0.4	O	S, PS	3, 10
2	Daikakuji	3520	172.31588	32.05762	1185	Y	21.8	1.2	47.5	0.3	O	S, PS	4, 10
3	Kammu	3480	172.82441	32.25556	467	P			43.7	0.3	O	PS	10
4	Unnamed	3442	173.14273	31.98011	422	P							
5	Abbott	3333	174.29323	31.80085	1660	Y	38.7	1.8	41.5	0.3	O	S, PS	7, 8
6	Unnamed	3178	175.68534	30.92440	1248	N							
7	Colahan	3162	175.89212	31.00839	258	P	38.6	0.6	38.7	0.2	O	R	7, 8
8	De Veuster	2987	177.57160	30.35817	717	P							
9	Hancock	2880	178.70814	30.26199	454	P					O	PS, R	
10	Townsend Cromwell	2829	179.08298	29.79075	373	P							
11	Unnamed	2801	179.33761	29.66935	630	P	27.4	1.0			O	PS	3
12	Helsley	2673	180.43604	28.88898	204	P			31.9	0.7	O	S	10
13	Unnamed	2631	180.86848	28.82517	473	P							
14	Academician Berg	2608	181.12843	28.84618	373	P	28.0	0.8	31.0	0.2	N	PS	3, 8
15	Turnif	2586	181.39030	28.90749	132	P			29.3	0.5	O	PS	10
16	Kure	2543	181.67311	28.42412	0	P							
17	Nero	2492	182.04716	27.96472	66	P							
18	Midway	2447	182.62606	28.23192	0	P	27.6	0.8	27.6	0.7	O	PS, S	9, 10
19	Ladd	2391	183.35274	28.52740	1276	P							
20	Pearl and Hermes	2293	184.14143	27.85638	8	P	20.6	1.0	24.7	0.2	O	PS	3, 10
21	Salmon Bank	2316	183.56190	26.94871	47	Y							
22	Kilo Moana	2114	185.46182	26.29606	62	Y							
23	Lisianski	2052	186.03035	26.05316	3	P							
24	Pioneer	1998	186.57755	26.00514	21	P					N	S, PS	
25	Kaiuli	1940	187.06600	25.64745	1036	Y							
26	West Northampton	1886	187.57849	25.51399	2	P							
27	East Northampton	1846	187.94182	25.36441	26	Y	20.7	1.2	26.6	5.4	N	S	5
28	Laysan	1831	188.26208	25.80226	25	P	20.7	0.8	19.9	0.6	N	S, PS	5
29	Mōlī	1795	188.59559	25.66337	1274	Y							
30	East Maro	1747	189.04887	25.54561	192	P							
31	West Maro	1682	189.63215	25.28332	526	P							
32	Raita	1611	190.52447	25.57851	15	Y							
33	Northwest Gardner	1514	191.47757	25.38959	1117	P							
34	Gardner	1449	191.99667	24.99779	0	P	12.3	2.0			N	S, PS	6
35	West St. Rogatien	1365	192.70846	24.58723	66	P							
36	St. Rogatien	1339	192.87269	24.33704	27	P							
37	West Brooks	1317	193.04847	24.20526	38	Y							
38	Brooks	1302	193.17582	24.11305	40	Y	13.0	1.2			N	PS	6
39	Southeast Brooks	1284	193.30334	23.98342	49	Y							
40	French Frigate	1230	193.78359	23.75517	0	Y	12.0	0.8			O	S	2
41	Kānehunamoku	1235	193.97006	24.29302	576	Y					N	PS	
42	Southeast French Frigate	1188	194.29549	23.91131	343	Y							
43	Mokumanamana	1080	195.29388	23.57299	0	Y	10.3	0.8			N	S, PS	2
44	Necker Southeast	1045	195.56861	23.37018	28	Y							
45	Keoea	963	196.41107	23.29043	416	Y							
46	West Twin Banks	920	196.82819	23.19820	61	Y	9.6	1.6			N	PS	6
47	East Twin Banks	901	197.06181	23.24395	13	Y							
48	Westpac Bank	871	197.38515	23.23252	344	Y							
49	West Nīhoa	825	197.75942	22.99400	31	Y					N	PS	
50	Nīhoa	794	198.16742	23.10350	0	Y	7.5	0.6			N	S	1, 2
51	Middle Bank	702	198.96032	22.71607	67	Y							

Note: mbsl—meters below sea level. Multibeam coverage: Y—yes; N—none; P—partial. All $^{40}Ar/^{39}Ar$ ages are relative to 28.02 Ma for the Fish Canyon sanidine standard. At several volcanoes, ages have been determined for both shield and post-shield lavas. Listed ages represent the oldest age (for shield stage, if available) or a weighted mean of multiple age determinations. XRF (X-ray fluorescence): O—old; N—new (this paper). Stage: S—shield; PS—postshield; R—rejuvenated. References: 1—Funkhouser et al., 1968; 2—Dalrymple et al., 1974; 3—Clague et al., 1975; 4—Dalrymple and Clague, 1976; 5—Dalrymple et al., 1981; 6—Garcia et al., 1987; 7—Duncan and Clague, 1984; 8—Sharp and Clague, 2006; 9—Dalrymple et al., 1977; 10—O'Connor et al., 2013.

also compiled the new names for several of these volcanoes using Google Earth, the GEBCO (General Bathymetric Chart of the Oceans; http://www.ngdc.noaa.gov/gazetteer/) database, and the Advisory Committee on Undersea Features database. Previous compilations, which were based on much less precise bathymetric data, found 53 (Bargar and Jackson, 1974; Clague and Dalrymple, 1987) to 63 volcanoes (Clague, 1996). Our new map (Fig. 1) is incomplete, especially in the northwestern part of the ridge where few multibeam surveys have been made. Thus, the identification of some seamounts was based on the global

estimated topography data (Smith and Sandwell, 1997) using Google Earth. The presence of Cretaceous seamounts along and near the Northwest Hawaiian Ridge (e.g., Wentworth, Castellano, and an unnamed seamount east of Salmon Bank; Clague et al., 1975; Garcia et al., 1987; O'Connor et al., 2013) complicates any attempt to make an accurate inventory of Northwest Hawaiian Ridge volcanoes without sampling each seamount. Only 27 seamounts in the Northwest Hawaiian Ridge have been sampled (Fig. 1; Table 1). Here we took a conservative approach in identifying volcanoes based on either new or previous sampling or multibeam data. Seamounts that are unsampled and poorly surveyed were considered part of the Hawaiian Ridge only if their summits are shallower than 1000 m below sea level and they are located along the trend of the ridge. More sampling and surveying is needed to determine with confidence whether seamounts along and near the axis of the Hawaiian-Emperor Chain are actually part of the Northwest Hawaiian Ridge or Cretaceous seamounts.

We identified 51 volcanoes between the bend in the Hawaiian-Emperor Chain (starting with Yuryaku) and the northern Hawaiian Islands (Middle Bank is the southernmost volcano; Table 1). The distance of each volcanic center from Kīlauea volcano (Table 1) was determined using the most recent and highest resolution global topographic database compilation (SRTM30_PLUS), which includes shipboard soundings derived from multibeam bathymetry and predicted topography for other unmapped regions using satellite gravity measurements (Becker et al., 2009). The center of Kīlauea's summit crater, Halema'uma'u, was chosen as the starting reference point (–155.273840°, 19.413017°). The data were gridded at 1 km spacing and imported into the visualization and analysis software package Fledermaus (http://www.qps.nl/display/fledermaus), which was used to determine the most likely locations of the volcanic centers. The coordinates were picked and then exported to the GMT (Generic Mapping Tools) System program map project (Wessel and Smith, 1991), which was used to measure the distance from Kīlauea to each volcanic center.

The Northwest Hawaiian Ridge volcanoes are characterized by their diversity in shape and size. Their configuration varies greatly, from small volcanoes with a conical shape (e.g., unnamed volcano southwest of Colahan) or star pattern of rift zones (Abbott) to a giant volcano with three massive rifts (Gardner; Fig. 1). Several of the volcanoes are strongly asymmetrical with one extraordinarily long rift (e.g., West St. Rogatien, West Northampton, and Pioneer; Fig. 1) similar to some volcanoes in the Hawaiian Islands (Haleakalā and Kīlauea). Some isolated volcanoes have more than three rift zones (e.g., Middle Bank, French Frigate, and Raita) like Kaua'i volcano. The size of Northwest Hawaiian Ridge volcanoes ranges from 54×10^3 km^3 (Gardner) to ~1×10^3 km^3 (Academician Berg; Bargar and Jackson, 1974). In comparison, the volcanoes of the Hawaiian Islands vary in volume from 74×10^3 km^3 (Mauna Loa) to 9.6×10^3 km^3 (Ka'ula; Robinson and Eakins, 2006). Not surprisingly, the magma flux for the Northwest Hawaiian Ridge is much lower than for the Hawaiian Islands (1–9 m^3 s^{-1} versus 8–16 m^3 s^{-1}; Vidal and Bonneville, 2004). There has been an exponential increase in magma flux over the past 5 m.y. (Fig. 2). Overall, there has been a progressive increase in magma flux along the Northwest Hawaiian Ridge starting ~500 km after the bend in the Hawaiian-Emperor Chain with a sharp flux increase for Gardner volcano (Fig. 2).

GEOCHRONOLOGY OF THE NORTHWEST HAWAIIAN RIDGE

Numerous radioisotopic ages were obtained in the 1960s to 1980s for volcanic samples collected during several dredging and drilling expeditions along the Hawaiian-Emperor Chain. These ages generally get progressively older with distance from the current location of the mantle plume beneath the Island of Hawai'i, supporting the hotspot hypothesis (Wilson, 1963; McDougall, 1971; Morgan, 1971). These early ages were generated using conventional K-Ar or ^{40}Ar/^{39}Ar total fusion techniques on large, porphyritic, whole-rock samples that are prone to potassium mobilization or may contain excess Ar. Moreover, K-Ar ages are model ages that assume trapped Ar has an atmospheric ^{40}Ar/^{36}Ar ratio, making the accuracy of these ages difficult to assess. In some compilations of K-Ar ages for multiple samples from one volcano, it was assumed that the oldest age was the best age (e.g., Clague and Dalrymple, 1987), although ages were averaged in other studies (e.g., Garcia et al., 1987).

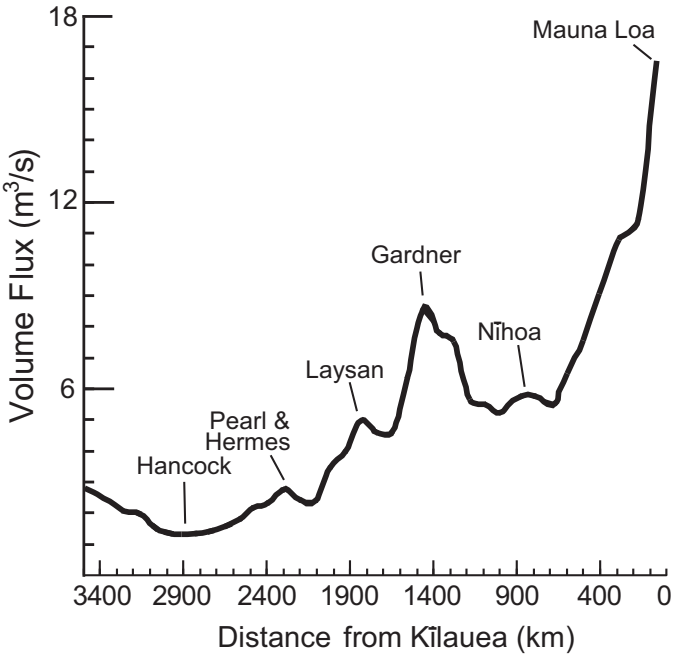

Figure 2. Temporal variation in the magma flux (m^3 s^{-1}) for the Hawaiian Ridge estimated using a flexural compensation model (modified after Vidal and Bonneville, 2004). Note the dramatic increase in flux toward the Hawaiian Islands, with Mauna Loa at the young end of the ridge, and the distinct high at Gardner. Other prominent volcanoes along the chain are labeled. No magma flux was estimated at the bend in the Hawaiian-Emperor Chain to avoid biased values due to the computation method used (Vidal and Bonneville, 2004).

High-precision, accurate age information is surprisingly sparse for the 2800-km-long Northwest Hawaiian Ridge from Middle Bank volcano to the bend. Although more than 50 K-Ar and total fusion $^{40}Ar/^{39}Ar$ ages (ranging from 30.7 ± 0.7 to 7.2 ± 0.3 Ma) exist for these volcanoes (Dalrymple et al., 1974, 1977, 1981; Dalrymple and Clague, 1976; Clague et al., 1975; Duncan and Clague, 1984; Garcia et al., 1987), these ages should be used with caution (Fig. 3). For example, the existing ages seem to indicate that an ~900 km section from Hancock to East Northampton volcanoes formed at the same time (ca. 27 Ma). Early $^{40}Ar/^{39}Ar$ incremental heating experiments, despite being conducted on whole-rock cores and consisting of 3–8 heating steps, yielded ages that were significantly (up to 20 m.y.) older than the K-Ar ages on the same samples (Fig. 3; Dalrymple and Clague, 1976; Dalrymple et al., 1981). However, these ages are also potentially problematic because whole-rock samples likely contain altered material and/or olivine phenocrysts, which invariably contain excess ^{40}Ar (Althaus et al., 2003).

The $^{40}Ar/^{39}Ar$ age determinations using modern techniques have been obtained from only 10 Northwest Hawaiian Ridge volcanoes, all west of 175°W (Sharp and Clague, 2006; O'Connor et al., 2013). Thus, more than half of the Hawaiian Ridge is devoid of modern geochronologic data. In comparison, 26 seamounts from the Louisville Chain in the south Pacific basin have high-precision $^{40}Ar/^{39}Ar$ ages (Koppers et al., 2004, 2011). Modern ages have been reported from shield and/or post-shield stage lavas on Yuryaku, Kammu, Daikakuji, and Abbott seamounts just south of the bend in the Hawaiian-Emperor Chain (Fig. 3). Only one $^{40}Ar/^{39}Ar$ age has been obtained for a Northwest Hawaiian Ridge rock that was interpreted to be from the rejuvenation stage (Colahan, 38.7 ± 0.2 Ma; Sharp and Clague, 2006). It is essential to consider the chemistry of the analyzed lavas when assessing

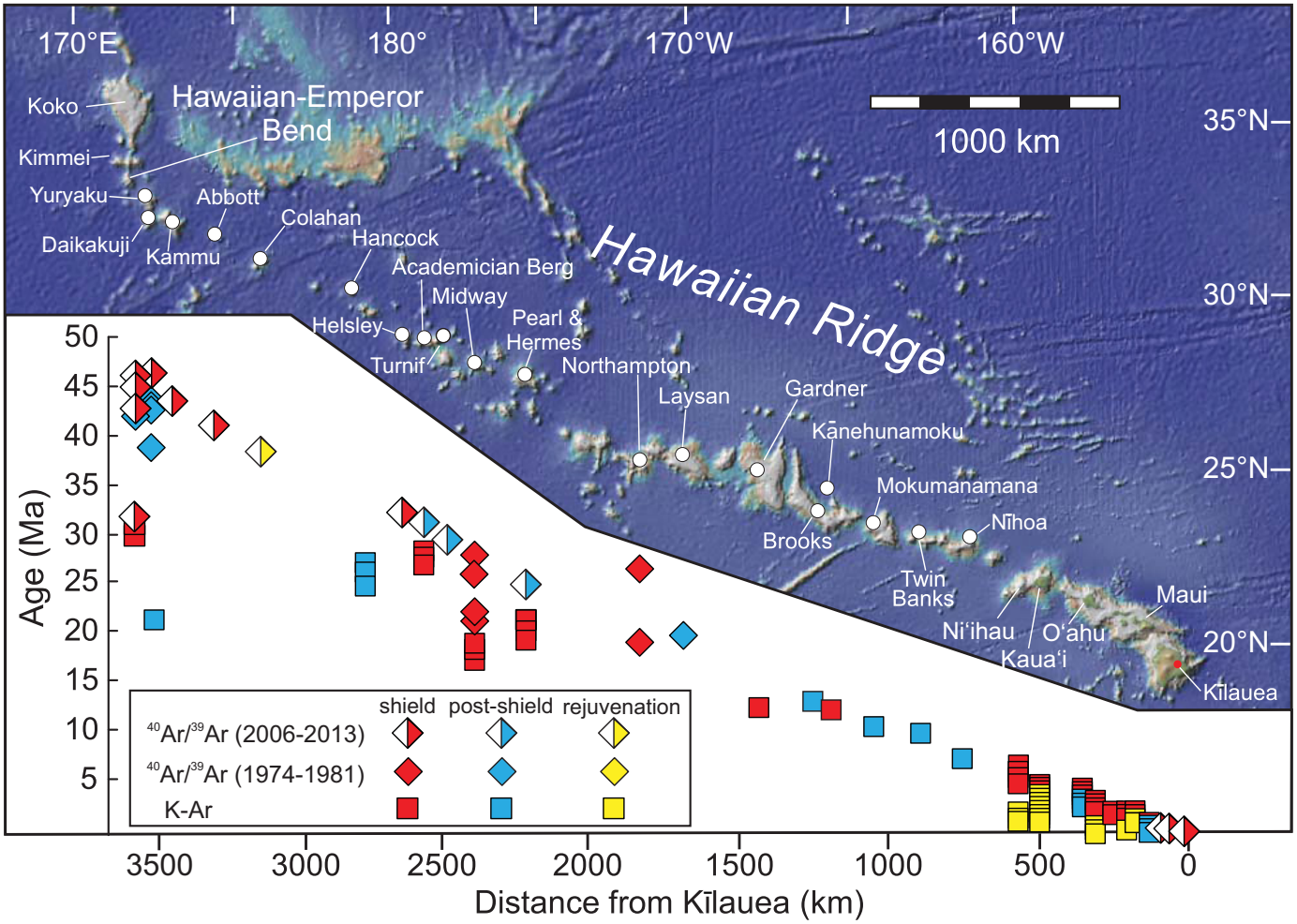

Figure 3. Map of the Hawaiian Ridge showing radiometric ages from Kīlauea to the Hawaiian-Emperor Bend. Only the volcanoes from the Island of Hawai'i and four near the bend have been dated by modern $^{40}Ar/^{39}Ar$ methods (half-filled diamonds; Sharp and Clague, 2006; Jicha et al., 2012; Sharp and Renne, 2005). The other ages were determined using K-Ar methods (squares) or $^{40}Ar/^{39}Ar$ with no separation of phenocrysts and few fusion steps (open diamonds). Data sources: Dalrymple et al. (1974, 1977, 1981), Clague et al. (1975), Dalrymple and Clague (1976), Clague and Dalrymple (1987), Garcia et al. (1987), Sherrod et al. (2007), O'Connor et al. (2013, and references therein). The ages are subdivided based on which eruptive stage of the volcano (shield—red; post-shield—blue, rejuvenation—yellow) was analyzed.

the progression of ages along the Hawaiian-Emperor Chain because geochronologic studies of the Hawaiian Islands have shown that rejuvenated volcanism may occur as much as 4 m.y. after the post-shield stage (e.g., Sherrod et al., 2007; Garcia et al., 2010). Thus, ages from rejuvenated lavas will not accurately reflect the timing of passage of the Pacific lithosphere over the plume vertical stem. Post-shield alkalic lavas may have double or more the potassium content of shield tholeiitic lavas and tend to yield more precise ages (e.g., Sharp and Renne, 2005). These lavas are probably erupted <0.5 m.y. after the shield stage (Garcia et al., 2007), and thus are desirable for determining reliable ages for Hawaiian volcanoes. The lack of $^{40}Ar/^{39}Ar$ ages determined by modern methods for much of the Northwest Hawaiian Ridge prevents the rate of Pacific plate motion to be well constrained during much of the Cenozoic (6 to 24 Ma).

SAMPLES AND PETROGRAPHY

We examined thin sections for 64 samples from 12 volcanoes along the Northwest Hawaiian Ridge. Modes for 26 representative samples are given in Table 2. Most of the samples (52) were collected by the *Pisces V* submersible from depths <2000 m (limit of submersible) and are labeled with the prefix P5. Two other sample suites were used: (1) dredged samples from the University of Hawai'i research expeditions in 1972 and 1976 (they are labeled with the prefix 72 or 76); and (2) samples from the islands of Mokumanamana (prefix NEC) and Nīhoa (prefix NIH) that were obtained from the University of California San Diego Scripps Collection. All of the studied samples have a manganese coating, which varied in thickness from <2 mm to >5 mm. There is no correlation between sample location along the chain and coating thickness. For example, East Northampton Seamount dredged samples (e.g., 76-5-4) have thin coatings (<1–2 mm), whereas submersible collected samples from neighboring Laysan Island volcano sample have thick coatings (~10 mm). Thinner coatings probably reflect more recent exposure to the surface rather than age of the sample.

The extent of sample alteration is highly variable (e.g., Gardner and Nīhoa volcanoes samples 76-6-7 and NIH-D-1-2, respectively, are weakly altered with only thin (<0.01 mm) iddingsite rims on olivine phenocrysts and open vesicles, whereas some samples (e.g., 72-37A from Gardner) have olivine that has been completely replaced by iddingsite and extensive development of secondary minerals (clay, zeolite, calcite, and/or phosphate filling vesicles and voids, and the glassy matrix is replaced by clays). Vesicularity in the ridge samples ranges widely from weak (~1 vol%; sample 76-5-4-A) to high (31%; sample P5-544-5 from Mokumanamana; Table 2). Many of the dredged samples have lower vesicularity (e.g., East Northampton, Gardner, and Brooks samples with <5 vol%; Table 2), perhaps related to eruption in deeper water (e.g., Moore, 1965). Vesicle shapes are commonly spherical, especially in the more vesicular samples.

Rock types vary from picritic basalt (>15 vol% olivine) to polymictic aphyric volcanic breccia (Table 2). Among the

TABLE 2. PETROGRAPHY OF SOME NORTHWEST HAWAIIAN RIDGE LAVAS BASED ON 300 POINT MODES

Volcano name	Sample number	Rock type	Mineralogy (vol% ph)			Vesicularity (vol%)	Alteration level
			Olivine	Cpx	Plag		
Academician Berg	72-20-CC	basanitoid	2	1	19	13	medium
Academician Berg	72-20-AA	alkalic basalt	3	2	11	18	medium
Pioneer	P5-524-2	tholeiite	3	4	9	21	medium
Pioneer	P5-524-3C	picrobasalt	4	–	–	16	medium
Pioneer	P5-524-4A	tholeiite	1	3	<1	12	low
Pioneer	P5-529-4	tholeiite	2	2	<1	2	low
East Northampton	76-5-4A	tholeiite	7	–	–	2	medium
Laysan	P5-530-1	trachyte	–	–	<1	1	low
Laysan	P5-530-3	alkalic basalt	2	2	3	3	medium
Raita	P5-538-1	tholeiite	1	1	10	1	medium
Gardner	76-6-7A	tholeiite	11	–	1	1	low
Gardner	72-37A	alkalic basalt	9+	–	<1	4	medium
Gardner	72-37C	alkalic basalt	8	<1	2	2	low
Brooks	72-41A	alkalic basalt	–	–	–	4	medium
Brooks	72-41B	alkalic basalt	3	–	–	2	medium
Mokumanamana	P5-543-3	mugearite	–	–	<1	8	low
Mokumanamana	P5-543-4	benmoreite	–	–	<1	22	medium
Mokumanamana	P5-544-1	benmoreite	–	–	<1	27	low
Mokumanamana	P5-544-4	trachyte	*	–	2	23	low
Mokumanamana	P5-544-5	trachyte	*	–	2	31	low
Mokumanamana	P5-544-6	benmoreite	<1	–	–	16	low
Mokumanamana	P5-544-7	trachyte	*	–	3	21	low
West Twin Banks	72-51A	basanitoid	–	–	–	4	medium
West Twin Banks	72-51B	basanitoid	<1	–	–	2	medium
West Nīhoa	76-9-11	alkalic basalt	30	–	–	12	low
Nīhoa	NIH-F-9	tholeiite	33	–	–	8	low

Note: Mineralogy reported only for phenocrysts (ph), >0.5 mm; Cpx—clinopyroxene, Plag—plagioclase. Alteration levels: low—minor alteration of olivine only; medium—extensive alteration of olivine and some clay or other minerals in vesicles and/or discoloration of matrix.

*Contains 2–3 vol% biotite and 1–5 vol% sanidine. +—olivine completely altered.

volcanic rocks, textures range from glassy to holocrystalline. Some samples have trachytic or felty textures, whereas others are intergranular or hyalopilitic. Olivine is the dominant phenocryst (<0.5 mm) with abundances from 0 to 33 vol% (Table 2). In the trachytic and felty textured samples, olivine is absent or rare (<1 vol%). Olivine preservation is excellent in some samples (e.g., from Nīhoa) and poor in others (totally replaced with clays and iron oxides; e.g., P5-529-1 from Pioneer Seamount). In samples with totally altered olivine, the clinopyroxene and plagioclase crystals are usually unaltered. Plagioclase phenocrysts are common (>4 vol%) in samples from Raita, Pioneer, and Academician Berg, but are otherwise sparse or absent in Northwest Hawaiian Ridge samples. Clinopyroxene phenocrysts are uncommon in these rocks (Table 2). Spinel occurs as inclusions in olivine, as groundmass crystals, and, rarely, as microphenocrysts (0.1–0.3 mm). Biotite was found in three Mokumanamana trachyte samples (Table 2).

WHOLE-ROCK MAJOR AND TRACE ELEMENT GEOCHEMISTRY

New XRF analyses were made of 45 samples from 12 volcanoes along the Northwest Hawaiian Ridge (Table 3). Samples were coarsely crushed (1–8 mm diameter) with a tungsten-carbide (WC) coated hydraulic press, ultrasonically cleaned in Millipore water, dried for 24 h at 40 °C and hand-picked to remove fragments with signs of alteration (discolored pieces and ones with minerals in vesicles). This procedure ensured that only the freshest parts of each sample were analyzed. Samples were powdered using a WC-lined mill. The P5 samples were analyzed at the University of Hawai'i (for analytical methods and precision for this laboratory, see Sinton et al., 2005). The other samples were analyzed at the University of Massachusetts (for analytical procedures and precision, see Rhodes and Vollinger, 2004). No samples were analyzed in both laboratories, but the BHVO-2 reference sample from Kīlauea volcano was run as an internal monitor in both laboratories and the results are comparable.

Alteration is a major concern for submarine samples older than 1 Ma. Although only the freshest material from each sample was analyzed by XRF, many of these samples have petrographic signs of alteration, as noted herein. Useful criteria for identifying altered rocks among the new analyses is high loss on ignition (LOI > 3 wt%) and P_2O_5 content (>2.5 wt%). Among the samples reported here, the LOI values are highly variable (<1–13 wt%; Table 3). Samples with LOI values >5 wt% were not included in the plots presented here. A few samples, especially evolved alkalic lavas from Laysan, have high P_2O_5 (compared to the highest value reported in Hawaiian Island basalts, 2.3 wt% from Kohala volcano; Spengler and Garcia, 1988). The presence of secondary phosphate in these samples was confirmed by petrographic inspection. Any sample with >3.1 wt% P_2O_5 was not included in the plots presented here. Another commonly used measure of alteration for Hawaiian tholeiitic lavas is K_2O/P_2O_5 (K/P), which is normally 1.5–2.0 in fresh tholeiitic lavas (e.g., Wright, 1971), although values as high as 3.2 have been reported in seemingly unaltered tholeiitic lavas from Mauna Kea volcano (Rhodes et al., 2012). The K/P ratio is highly sensitive to alteration. It reaches values as low as 0.4 among younger than 1 Ma, mildly altered lavas from the Hawaiian Scientific Drilling Project (Rhodes et al., 2012). For alkalic lavas, K/P is more variable even in fresh lavas, especially fractionated post-shield lavas (e.g., 0.7–4.7; Spengler and Garcia, 1988). Among the Northwest Hawaiian Ridge tholeiitic lavas, K/P varies from 0.5 to 1.8. However, many samples containing only weakly altered olivine (e.g., 76-6-7-A) have low K/P (<1), so they were included in all plots.

The new XRF major element analyses for Northwest Hawaiian Ridge lavas show a wide range in composition, from picrobasalt to trachyte (44–63.5 wt% SiO_2; Fig. 4). Tholeiitic basalts (samples that plot below the Macdonald-Katsura line on the TAS plot; Fig. 4) were obtained from Pioneer, Gardner, East Northampton, Laysan, Mokumanamana, and Nīhoa volcanoes. These compositions are diagnostic of the Hawaiian shield stage of volcanism (e.g., Macdonald et al., 1983). The tholeiitic samples vary markedly in MgO content (0.5–20.4 wt%; Table 3). Some samples (from Twin Banks, Pioneer, and Gardner) have transitional compositions plotting close to the dividing line on the TAS plot (Fig. 4). Transitional compositions are typical of the early post-shield stage of Hawaiian volcanism (e.g., Frey et al., 1990). The other new samples are basanitoids (no modal nepheline), alkalic basalts, or evolved alkalic lavas (hawaiite to trachyte; Fig. 4). Of the 12 sampled volcanoes, 4 have both tholeiitic and alkalic lavas (Mokumanamana, Gardner, Laysan, and Pioneer; Fig. 4). On MgO variation diagrams (Fig. 5), the samples show a linear increase in Al_2O_3 with decreasing MgO (a trend commonly observed in Hawaiian lavas; Jackson et al., 2012). This trend indicates that plagioclase has not played an important role in the fractionation history of these lavas. TiO_2 also shows an increasing trend with decreasing MgO, but only in rocks with MgO >3 wt%. Below that value, TiO_2 drops sharply from 4.6 to 0.6 wt% (Fig. 5). Total iron shows a similar trend (Table 3). The sharp decreases in TiO_2 and total iron probably indicate the crystallization of titaniferous magnetite, which occurs as microphenocrysts in these strongly evolved rocks. The CaO/Al_2O_3 ratio is high (0.8–1.0) for rocks with >6 wt% MgO (indicating dominance of olivine fractionation) but drops to 0.1 wt% in the low MgO samples (Fig. 5), reflecting extensive clinopyroxene fractionation.

Trace element concentrations in the Northwest Hawaiian Ridge samples are also highly variable, especially for compatible elements (Ni, 4–1086 ppm; Cr, 4–1166; Table 3), with the highest values in the olivine-rich tholeiites from Nīhoa, Gardner, and Pioneer volcanoes and lowest in the trachytes. Incompatible elements also show wide ranges in abundances (Ba, 32–2467 ppm; Sr, 113–1238 ppm; Table 3). Enrichment factors vary from 10 for Sr to >70 for Rb (which is highly susceptible to alteration artificially creating a high enrichment factor). Variation diagrams were made with Ba on the *x*-axis (which has an enrichment factor of 30). These plots generally show positive trends for Nb and Sr below 600 ppm Ba. The more evolved lavas from Mokumanamana

TABLE 3. WHOLE-ROCK X-RAY FLUORESCENCE ANALYSES FOR NORTHWEST HAWAIIAN RIDGE ROCKS

Seamount	Sample	SiO_2	TiO_2	Al_2O_3	Fe_2O_3*	MnO	MgO	CaO	Na_2O	K_2O	P_2O_5	Total	LOI	Rb	Ba	Nb	La	Ce	Sr	Zr	Y	Zn	Ni	Cr	V	Lab†
Academician Berg	72-20-AA	49.43	2.76	17.11	11.39	0.13	4.32	10.10	3.56	0.98	0.44	100.22	2.22	14.2	334	28.9	17	42	578	154	29.3	126	118	145	242	UM
Academician Berg	72-20-CC	43.31	5.08	15.91	16.43	0.29	3.12	9.34	3.56	1.31	1.37	99.72	1.75	17.4	509	54.9	48	119	1238	326	38.8	154	100	56	275	UM
Academician Berg	72-20-FF	46.31	3.15	12.92	13.67	0.17	8.20	10.81	2.80	1.02	0.50	99.56	3.98	16.9	281	36.9	26	66	520	240	27.9	136	357	397	246	UM
Pioneer	P5-524-2	47.44	2.73	14.02	14.42	0.20	7.49	10.42	1.99	0.44	0.36	99.49	4.01	5.0	44	15.1	nd	nd	349	156	258	268	881	911	308	UH
Pioneer	P5-524-3C	44.42	3.04	13.18	14.54	0.26	7.22	12.57	1.78	0.40	0.44	97.85	2.89	5.5	114	19.2	nd	nd	369	188	31.8	139	275	578	344	UH
Pioneer	P5-524-4A	46.64	3.46	15.44	14.49	0.37	6.59	10.44	2.00	0.64	0.42	100.48	3.18	6.4	44	22.5	nd	nd	374	211	30.0	148	320	404	363	UH
Pioneer	P5-525-2	47.19	3.32	13.79	13.94	0.19	6.11	11.45	2.06	0.54	0.81	99.37	1.61	7.9	36	19.8	nd	nd	370	190	39.6	150	120	82	360	UH
Pioneer	P5-527-1	48.87	3.26	16.23	14.05	0.18	4.14	7.72	3.34	1.29	1.12	100.17	1.69	19.5	229	42.0	nd	nd	744	521	61.5	220	19	nd	168	UH
Pioneer	P5-529-1	44.27	3.17	14.28	14.48	0.19	5.52	13.99	1.91	0.45	2.25	100.52	2.80	7.5	57	22.1	nd	nd	473	196	85.7	193	113	657	384	UH
Pioneer	P5-529-3	43.38	3.09	13.35	12.92	0.15	6.23	15.97	1.65	0.42	2.96	100.09	1.91	7.2	54	19.5	nd	nd	501	178	89.1	155	108	469	345	UH
Pioneer	P5-529-4	47.09	3.44	15.31	14.48	0.17	5.15	11.71	1.90	0.38	0.78	100.40	1.19	5.7	56	22.6	nd	nd	444	211	59.8	169	92	244	390	UH
East Northampton	76-5-4-A	48.63	2.33	12.12	12.63	0.18	11.39	10.22	1.96	0.26	0.23	99.95	1.24	3.4	83	12.8	8	26	300	142	23.1	113	332	924	253	UM
Laysan	P5-530-1	63.46	0.64	17.46	4.44	0.12	1.20	2.03	5.64	4.64	0.08	99.69	0.85	105	443	127.1	nd	nd	113	457	59.2	128	109	100	71	UH
Laysan	P5-530-2	63.22	0.63	17.50	4.37	0.09	0.98	1.67	5.83	4.96	0.09	99.32	0.91	105	454	124.9	nd	nd	114	448	52.9	110	83	100	57	UH
Laysan	P5-530-3	47.62	2.72	15.38	13.37	0.15	5.85	12.40	1.81	0.54	0.28	100.12	1.43	7.4	140	16.4	nd	nd	434	147	75.6	118	86	166	383	UH
Raita	P5-538-1	46.24	4.64	15.95	12.85	0.16	4.32	9.69	2.71	1.90	1.03	99.49	2.56	35.3	455	58.0	nd	nd	1093	441	43.7	151	26	nd	329	UH
Gardner	72-37-A	45.80	2.34	15.07	13.09	0.18	10.05	9.97	2.55	0.59	0.36	100.01	2.12	7.6	300	27.6	15	36	533	128	25.0	80	188	507	204	UM
Gardner	72-37-C	45.89	2.34	15.03	13.17	0.18	10.12	10.02	2.57	0.56	0.36	100.23	2.09	6.6	325	28.2	13	38	539	130	25.2	81	173	508	215	UM
Gardner	76-6-7-A	47.19	1.71	10.70	12.51	0.18	16.62	8.85	1.68	0.14	0.17	99.75	1.17	1.1	65	9.3	4	18	218	101	18.8	102	626	1032	219	UM
Gardner	76-6-7-B	47.61	1.78	10.93	12.48	0.18	16.09	9.10	1.73	0.13	0.17	100.20	1.48	0.8	60	10.1	4	23	218	104	19.8	103	650	1142	226	UM
Gardner	76-6-7-C	47.31	1.78	11.03	12.53	0.18	15.42	9.21	1.75	0.18	0.17	99.55	1.55	1.4	75	9.7	5	22	228	107	20.0	105	576	989	239	UM
Gardner	76-6-7-D	47.56	1.77	11.01	12.66	0.18	16.02	9.10	1.73	0.13	0.17	100.32	1.57	0.9	67	9.6	4	21	220	104	19.6	102	607	1049	223	UM
Gardner	76-6-7-F	47.19	1.72	10.79	12.64	0.18	16.73	8.91	1.70	0.13	0.17	100.15	1.17	0.4	68	9.3	9	22	216	101	19.2	102	629	1060	222	UM
Brooks	72-41-A	46.36	4.07	15.67	14.42	0.22	5.00	8.78	3.48	1.27	0.65	99.91	1.73	21.5	399	42.6	28	71	738	302	38.0	125	4	4	264	UM
Brooks	72-41-B	45.92	2.35	14.92	13.20	0.18	10.14	9.98	2.58	0.62	0.36	100.24	2.03	8.1	314	28.4	18	39	535	131	25.6	83	175	504	218	UM
Kānehunamoku	P5-695-1	43.88	5.45	15.99	15.18	0.90	4.53	9.54	2.25	0.96	1.03	99.72	4.83	6.3	2467	31.7	35	44	687	370	61.8	181	522	250	315	UM
Kānehunamoku	P5-701-2	45.89	3.12	12.64	14.34	0.17	8.84	11.09	2.42	0.81	0.40	99.72	1.02	17.0	319	39.5	31	86	723	389	42.5	172	51	34	292	UM
Kānehunamoku	P5-701-4	49.55	4.35	15.86	10.09	0.15	4.44	9.65	3.88	1.43	0.78	100.18	1.54	21.0	185	22.3	16	45	469	213	26.6	131	282	661	274	UM
Mokumanamana	NEC 3A	46.38	2.29	9.43	14.04	0.18	17.04	8.34	1.31	0.45	0.50	99.95	1.79	4.2	127	15.6	17	40	251	156	47.6	135	664	1166	22	UM
Mokumanamana	P5-543-3	51.66	2.15	18.19	11.03	0.13	0.96	6.12	4.84	2.51	1.81	99.37	1.98	24.4	622	70.5	nd	nd	1154	578	77.0	218	37	6	162	UH
Mokumanamana	P5-543-4	55.84	1.32	19.75	7.71	0.16	1.53	4.41	5.32	2.41	1.06	99.51	4.37	20.0	825	84.3	nd	nd	1144	603	128	220	43	nd	39	UH
Mokumanamana	P5-544-1	60.04	1.01	18.70	5.54	0.16	1.36	2.98	5.64	3.30	0.66	99.37	3.24	46.4	868	94.8	nd	nd	979	894	70.9	227	26	nd	10	UH
Mokumanamana	P5-544-4	61.47	0.83	19.14	4.44	0.17	0.37	2.28	6.24	4.11	0.47	99.52	0.71	55.7	994	100.6	nd	nd	849	591	50.0	155	91	nd	41	UH
Mokumanamana	P5-544-5	60.61	0.86	19.43	4.83	0.18	0.60	2.41	6.24	3.67	0.48	99.30	2.00	30.3	1083	75.8	nd	nd	910	363	46.1	150	56	nd	9	UH
Mokumanamana	P5-544-6	59.42	0.98	19.05	5.61	0.18	1.47	3.06	5.57	3.25	0.79	99.38	2.48	45.4	886	100.0	nd	nd	974	970	75.3	223	23	nd	12	UH
Mokumanamana	P5-544-7	60.99	0.83	19.16	4.59	0.16	0.49	2.31	6.29	3.96	0.50	99.26	0.96	39.9	998	92.7	nd	nd	863	576	51.4	143	38	nd	29	UH
West Twin Banks	72-51-A	43.67	3.98	13.39	16.31	0.21	5.97	9.23	3.38	0.82	3.08	100.04	3.36	7.8	213	34.9	36	109	825	360	70.6	228	20	10	154	UM
West Twin Banks	72-51-B	43.89	4.03	13.48	16.09	0.20	5.56	9.23	3.39	0.90	3.09	99.86	1.03	9.0	195	35.4	35	116	819	364	71.3	242	22	6	153	UM
West Twin Banks	72-51-C	43.93	3.99	13.43	16.15	0.20	5.53	9.21	3.36	0.88	3.08	99.77	0.82	8.7	206	35.2	38	112	825	363	71.8	238	21	6	158	UM
West Twin Banks	72-51-D	43.85	3.94	13.38	16.29	0.21	5.70	9.21	3.32	1.10	3.05	100.04	1.06	12.7	205	35.0	33	108	824	357	70.5	229	20	12	153	UM
West Twin Banks	72-51-E	43.74	3.98	13.31	16.28	0.21	5.66	9.24	3.34	0.88	3.05	99.69	0.99	9.0	197	35.0	34	113	815	358	70.6	235	22	7	156	UM
West Twin Banks	P5-688-1	43.54	1.99	9.93	14.52	0.19	16.24	10.27	1.48	0.21	1.38	99.75	1.33	2.9	32	9.7	6	19	283	117	24.2	156	635	909	249	UM
West Nīhoa	72-9-11	45.79	2.49	10.45	14.22	0.20	16.24	7.20	2.11	0.68	0.37	99.75	1.33	8.2	114	17.7	9	37	395	179	21.5	165	669	806	193	UM
Nīhoa	NIH-F-9	46.28	1.87	8.90	13.02	0.17	20.45	7.21	1.61	0.21	0.31	100.03	3.49	2.2	69	11.3	14	24	286	129	18.5	130	1086	1072	187	UM
Nīhoa	NIH-D-1-2	47.57	2.58	9.89	13.34	0.17	15.37	7.77	2.05	0.63	0.37	99.73	0.42	9.3	171	19.6	23	50	505	198	22.1	130	684	792	212	UM

Note: Major elements are in weight percent; trace elements are in parts per million; LOI—loss on ignition; nd—not determined.
*Total iron.
†Lab—laboratory for X-ray fluorescence: UH—University of Hawai'i; UM—University of Massachusetts.

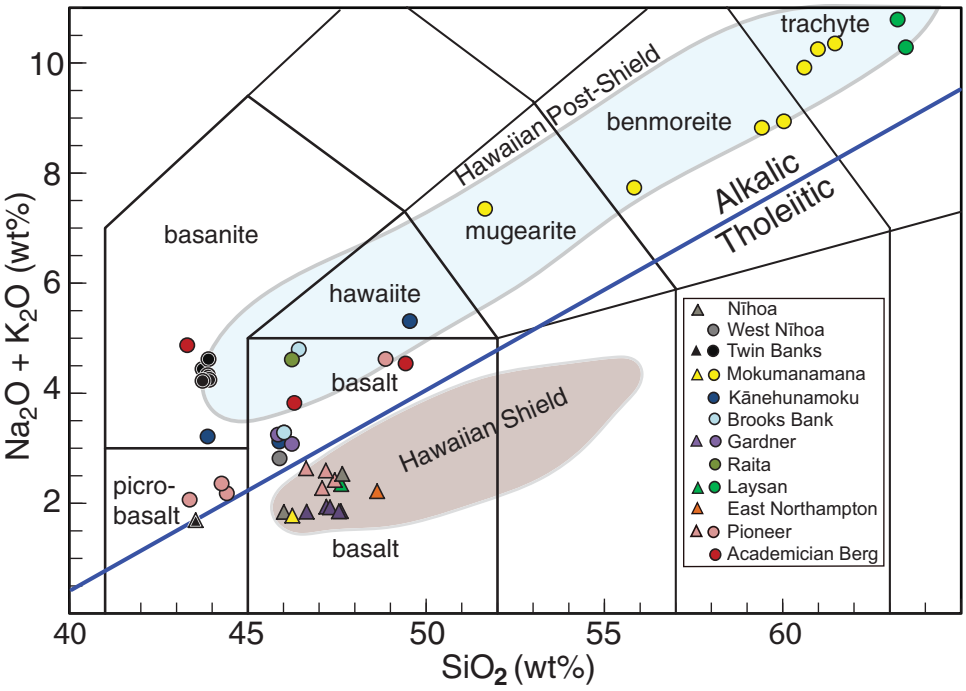

Figure 4. Total alkalies versus silica plot with the rock classification scheme of Le Maître (2002) for new X-ray fluorescence (XRF) analyses of lavas from the Northwest Hawaiian Ridge (from data in Table 3). The blue dividing line for separating alkalic (circles above the line) from tholeiitic lavas (triangles below) is from Macdonald and Katsura (1964). The new samples include tholeiitic basalts from Nīhoa, Twin Banks, Gardner, East Northampton, Laysan, and Pioneer, and alkalic basalts from all 12 sampled volcanoes except Nīhoa and East Northampton. Fields for alkalic (light blue) and tholeiitic lavas (mauve) from the Hawaiian Islands are from Clague and Sherrod (2014). Two σ errors are smaller than the symbol size.

are off the trend (Fig. 6), perhaps related to fractionation of alkali feldspar, which is present in these samples (Table 2). Plots of incompatible elements ratios (Zr/Nb, Nb/Y) versus Ba show more scattered trends, especially for the trachytes (Fig. 6). Zr/Nb ratios are <14 in all samples, which is typical of lavas from Kea trend volcanoes (e.g., Kīlauea and Mauna Kea; Quane et al., 2000; Rhodes et al., 2012).

One method that has been used to distinguish Hawaiian alkalic lavas from post-shield versus rejuvenation stages is a plot of Nb/Y versus Zr/Y. Fitton (2007) and Greene et al. (2010) showed that shield lavas plot slightly below and at angle to the Δ Nb = 0 line, post-shield alkalic lavas plot somewhat above this trend with higher Nb/Y values, and rejuvenated rocks plot well above both groups with the highest Nb/Y values for a given Zr/Y (Fig. 7). Among our new samples, the ones with tholeiitic and transitional compositions plot within or along the Hawaiian shield trend, whereas some samples from Laysan, Gardner, Mokumanamana, and Brooks Banks volcanoes plot in or near the field for rejuvenated lavas (Fig. 7). Similar samples from Academician Berg Seamount were dated by $^{40}Ar/^{39}Ar$ and interpreted to be post-shield lavas (Sharp and Clague, 2006). The Laysan samples are benmoreites and trachytes; these rocky types have been reported only among post-shield sequences for Hawaiian volcanoes (Macdonald et al., 1983) and never from rejuvenated suites (e.g., Kauai; Garcia et al., 2010). A sample from Brooks Bank (72–41B) plots in the rejuvenated field (Fig. 7), although it is a weakly alkalic basalt, unlike most rejuvenated lavas. The K-Ar age for this sample is ~3 m.y. younger than the alkalic basalt dated sample from this volcano (Garcia et al., 1987), so it might be a rejuvenated rock. Modern ^{40}Ar-^{39}Ar ages and Sr and Nd isotope analyzes are needed to assess its stage of volcanism as post-shield or rejuvenated lavas. Rejuvenated lavas are younger and are derived from more depleted sources (i.e., lower $^{87}Sr/^{86}Sr$ and higher $^{143}Nd/^{144}Nd$) than post-shield lavas in Hawai'i (e.g., Frey et al., 2005).

Pb, Sr, Nd, AND Hf ISOTOPIC VARIATION

Isotopes, including Pb, Hf, Nd, and Sr, provide a powerful method of evaluating the mantle source, magmatic processes, and melt history of volcanic rocks (e.g., Hofmann, 2003; Weis et al., 2011). Study of the isotopic characteristics of Northwest Hawaiian Ridge lavas began with strontium isotopes (Lanphere et al., 1980). Only two subsequent isotope studies have followed this pioneering work on the ridge (Basu and Faggart, 1996; Regelous et al., 2003). High-precision modern isotopic data are even scarcer with only four samples from the two oldest Hawaiian Ridge seamounts, Daikakuji and Yuryaku (Regelous et al., 2003). There are no Hf isotope data for the entire Northwest Hawaiian Ridge, although this system is paramount in documenting the presence of recycled material in the source of Hawaiian basalts (e.g., Blichert-Toft et al., 1999).

Alteration and contamination of samples radically affects the subsequent measured isotopic values of samples (e.g., Abouchami et al., 2005; Nobre-Silva et al., 2009, 2010). In order to achieve accurate isotopic measurements on altered submarine basalts, acid leaching is essential. This is especially true for Pb and Sr, which are susceptible to post-eruption mobility and contamination from Fe-Mn crusts for Pb (Abouchami et al., 2005; Nobre Silva et al., 2009) or seawater for Sr (Zindler et al., 1984). Furthermore, in order to correct isotopic measurements to the initial

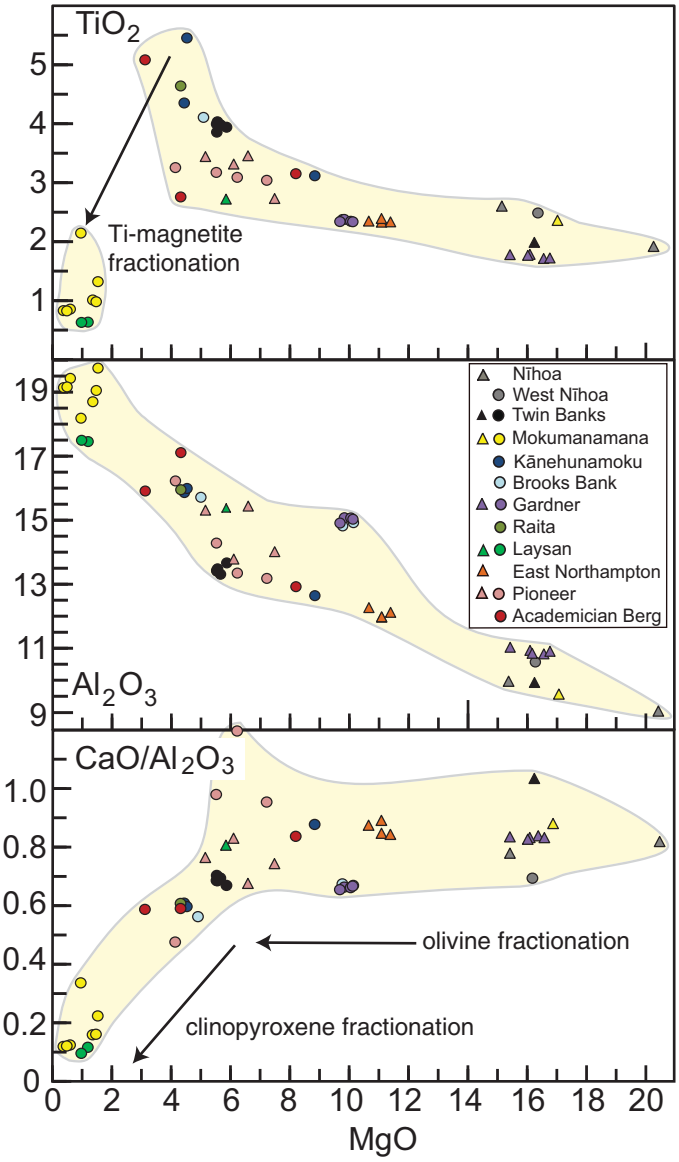

Figure 5. MgO variation plots for TiO_2, Al_2O_3, and CaO/Al_2O_3 (all in wt%) for new X-ray fluorescence analyses of lavas from the Northwest Hawaiian Ridge (from data in Table 3). There are wide ranges in MgO for tholeiites (triangles; 5–20 wt%) and alkalic lavas (circles; 0.4–16 wt%). TiO_2 increases markedly with decreasing MgO (especially from 6 to 3 wt% MgO), and drops markedly for the lowest MgO samples (<2 wt%), probably related to fractionation of Ti-rich magnetite. Al_2O_3 increases steadily with decreasing MgO despite the presence of plagioclase phenocrysts in many of the lower MgO samples. The high CaO/Al_2O_3 ratios of lavas with >5 wt% MgO (although variable for the alkalic lavas) suggest that olivine is the dominant fractionating phase. The lower CaO/Al_2O_3 in the lower MgO samples indicates that clinopyroxene has been important in their crystallization history. Two σ errors are smaller than the symbol size.

magmatic values both accurate ages and radiogenic isotope parent element concentrations are required. We have discussed the problems with reliable radiometric ages for Northwest Hawaiian Ridge lavas. There are also difficulties in obtaining primary elemental concentrations of parent-daughter elements, undisturbed by secondary alteration, because some elements (e.g., U, Rb, and, to a lesser extent, Pb) are highly susceptible to low-temperature alteration. Thus, the measured elemental concentrations in weakly altered submarine basalts are usually not representative of the primary parent-daughter concentration, resulting in poor corrections of the measured isotopic ratios for post-eruption *in situ* decay. Careful selection of average oceanic island basalt normalization ratios can be used to correct this problem, although the results still include considerable uncertainty that may account for some erroneous values in data sets (e.g., Regelous et al., 2003). The reliability of the existing isotopic database for the Northwest Hawaiian Ridge is strongly compromised by the uncertainties associated with inadequate treatment of these problems.

Here we present a compilation of Sr, Nd, Pb, and Hf isotopic data for the Emperor Seamounts and Northwest Hawaiian Ridge (Table A1 in Appendix). The database includes samples without acid leaching and/or age correction for in situ decay; otherwise too few samples would remain to be considered. Emperor Seamount samples that were overcorrected for age, as identified by unreasonable $^{208}Pb^*/^{206}Pb^*$ values (where $^{208}Pb^*/^{206}Pb^* = [^{208}Pb/^{204}Pb - 29.475]/[^{206}Pb/^{204}Pb - 9.306]$; Hofmann, 2003) were removed, and no attempt was made to correct isotope data already corrected to pre-1990 ages to more current ages because too few modern ages exist. All data were normalized to the same standard values to ensure comparability between laboratories: Nd isotopic ratios were normalized to a $^{143}Nd/^{144}Nd$ La Jolla value of 0.511858 or a Rennes value of 0.511973; Sr isotopic ratios were normalized to an $^{87}Sr/^{86}Sr$ SRM 987 value of 0.710248; Pb isotopic ratios were normalized to SRM 981 values of 16.9405 for $^{206}Pb/^{204}Pb$, 15.4963 for $^{207}Pb/^{204}Pb$, and 36.7219 for $^{208}Pb/^{204}Pb$, and Hf isotopic ratios were normalized to a $^{176}Hf/^{177}Hf$ JMC 475 value of 0.282160 (e.g., Weis et al., 2006). We used present-day CHUR (chondritic uniform reservoir) values of $^{143}Nd/^{144}Nd = 0.512638$ and $^{176}Hf/^{177}Hf = 0.282772$ to calculate ε_{Nd} and ε_{Hf}, respectively. The closest known age or inferred age was used to calculate ε_{Nd} and ε_{Hf} values (Table A1 in Appendix).

The available Sr and Nd isotopic data along the Northwest Hawaiian Ridge are nearly homogeneous without any robust trends (Fig. 8). The ε_{Nd} values are relatively high from the Emperor Seamounts through the Northwest Hawaiian Ridge compared to the values for the Hawaiian Islands (Fig. 8B). There is a slight decrease in ε_{Nd} values from Gardner to Nīhoa volcanoes, although the values for Daikakuji (near the bend in the Hawaiian-Emperor Chain) are lower (Fig. 8B). Sr isotopic ratios span a broad range for the Hawaiian Ridge with no consistent trend versus distance from Kīlauea (Fig. 8A). Some individual volcanoes show broad ranges (e.g., Daikakuji for two transitional basalts), whereas others have a narrow range in Sr isotopic ratios (Gardner and Mokumanamana) that may reflect limited data. The lack of step-wise acid leaching to remove secondary material (e.g., Nobre Silva et al., 2009, 2010) for the Basu and Faggart (1996) data set

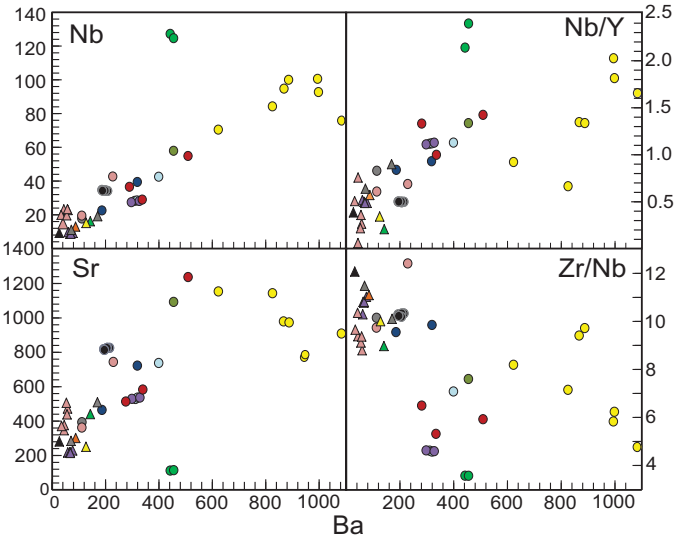

Figure 6. Trace element variation plots for Ba versus Sr, Nb, Nb/Y, and Zr/Nb for new XRF analyses of lavas from the Northwest Hawaiian Ridge (from data in Table 3). Ba, Sr, and Nb values are in ppm. A good positive trend was found for Nb versus Ba, but trends are more scattered for Sr and Nb/Y and Zr/Nb ratios, especially for the trachytes from Laysan and Mokumanamana. The two Laysan trachyte samples (green circles) have anomalously low Ba contents compared to the Mokumanamana trachytes. Two σ errors are smaller than the symbol size.

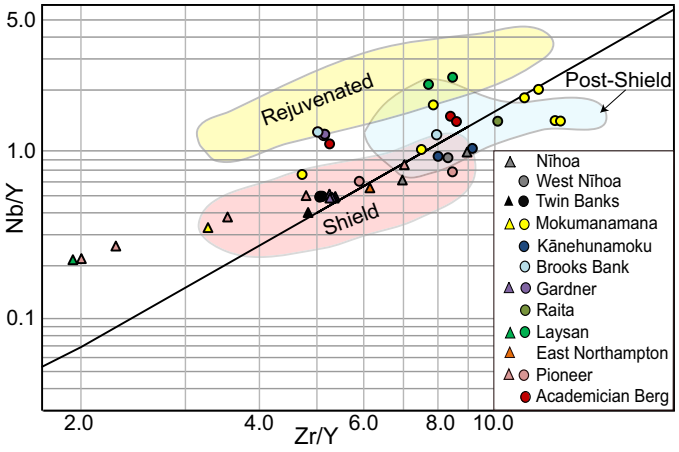

Figure 7. Plot of Nb/Y versus Zr/Y for lavas from the Northwest Hawaiian Ridge (from data in Table 3) after Fitton et al. (1997). The diagonal line is the Δ Nb = 0 reference line of Fitton (2007), which separates the fields for Icelandic and normal mid-oceanic ridge basalt (N-MORB) lavas. Fields for Hawaiian shield and rejuvenated lavas are from Greene et al. (2010), and include the two best-known examples of rejuvenated volcanism from Honolulu Volcanics of Oahʻu and the Kōloa Volcanics from Kauaʻi. The post-shield field is inferred from results for Maui post-shield lavas (Fitton, 2007).

compromises rigorous interpretation of their isotopic data. The $^{87}Sr/^{86}Sr$ isotopic ratios for rocks from the Emperor Seamounts progressively increase (0.70295–0.70370) from the oldest seamount, Meiji, southward to the bend (Fig. 8A) as shown previously (Regelous et al., 2003; Frey et al., 2005). Most Sr and Nd isotopic ratios of Northwest Hawaiian Ridge lavas are Kea-like, with lower $^{87}Sr/^{86}Sr$ (0.70335–0.70408) and higher ε_{Nd} (5.7–8.7; Fig. 8), in comparison to the data set on the Hawaiian Islands (e.g., Tanaka et al., 2008). Post-shield type, weakly alkalic Northwest Hawaiian Ridge lavas overlap in Sr and Nd isotopic ratios with shield-like tholeiitic lavas from the same volcanoes (Fig. 8). In contrast, Sr isotopic ratios in shield lavas from Hawaiian Island volcanoes are higher than those from post-shield lavas, which overall show more depleted isotopic characteristics (low $^{87}Sr/^{86}Sr$, high $^{143}Nd/^{144}Nd$ and $^{176}Hf/^{177}Hf$, and unradiogenic Pb; e.g., Hanano et al., 2010). It is important to note that the Sr isotopic measurements for samples from the Northwest Hawaiian Ridge probably do not represent magmatic values due to the lack of acid leaching; therefore, we report these results with caution.

There are virtually no Pb isotope data available for the Northwest Hawaiian Ridge except for the two oldest volcanoes, Yuryaku and Daikakuji (Regelous et al., 2003). Two Daikakuji basalts have unradiogenic Pb isotopic ratios, with $^{206}Pb/^{204}Pb$ as low as 17.97, typical of Loa trend volcanoes from the Hawaiian Islands (Fig. 9). The one sample analyzed from Yuryaku has higher $^{206}Pb/^{204}Pb$, typical of Kea-type lavas (Fig. 9). These three lavas are transitional basalts with Kea-like major and trace element compositions.

DISCUSSION

Stages of Volcanism

The new XRF results (Table 3) confirm the presence of shield and post-shield volcanism on many Northwest Hawaiian Ridge volcanoes. Tholeiitic rocks are present on the islands with erosional remnants of shield volcanoes (Nīhoa, Mokumanamana, French Frigate, and Gardner volcanoes), were dredged from several other volcanoes (e.g., Yuryaku, Daikakuji, Pioneer, Nero, and Abbott), and drilled from Midway (Clague and Dalrymple, 1989). The presence of tholeiitic lavas along the entire length of the Hawaiian Ridge is notable because some other oceanic island chains with lower magma supply rates apparently lack tholeiitic lavas (e.g., Louisville Ridge; Vanderklusyen et al., 2014). Most of the Northwest Hawaiian Ridge volcanoes with tholeiitic lavas are moderate to large volcanoes (10–54 × 10^3 km^3), although Nero and East Northampton are smaller volcanoes (4 and 7 × 10^3 km^3; Bargar and Jackson, 1974). Therefore, shield stage tholeiitic lavas have been recovered from nearly the full length of the Northwest Hawaiian Ridge and from small to large volcanoes. Tholeiitic lavas also have been recovered from several of the Emperor Seamounts (e.g., Regelous et al., 2003; Duncan and Keller, 2004). Lavas with compositions typical of the post-shield stage (transitional and alkalic basalts, and moderately to highly evolved alkalic lavas) are common on many of the Northwest Hawaiian Ridge volcanoes and along its entire length (West Nīhoa to Yuryaku; Tables 1 and 3). Thus, the Northwest Hawaiian Ridge volcanoes continue the same evolutionary compositional trend that is well documented for the Hawaiian Islands

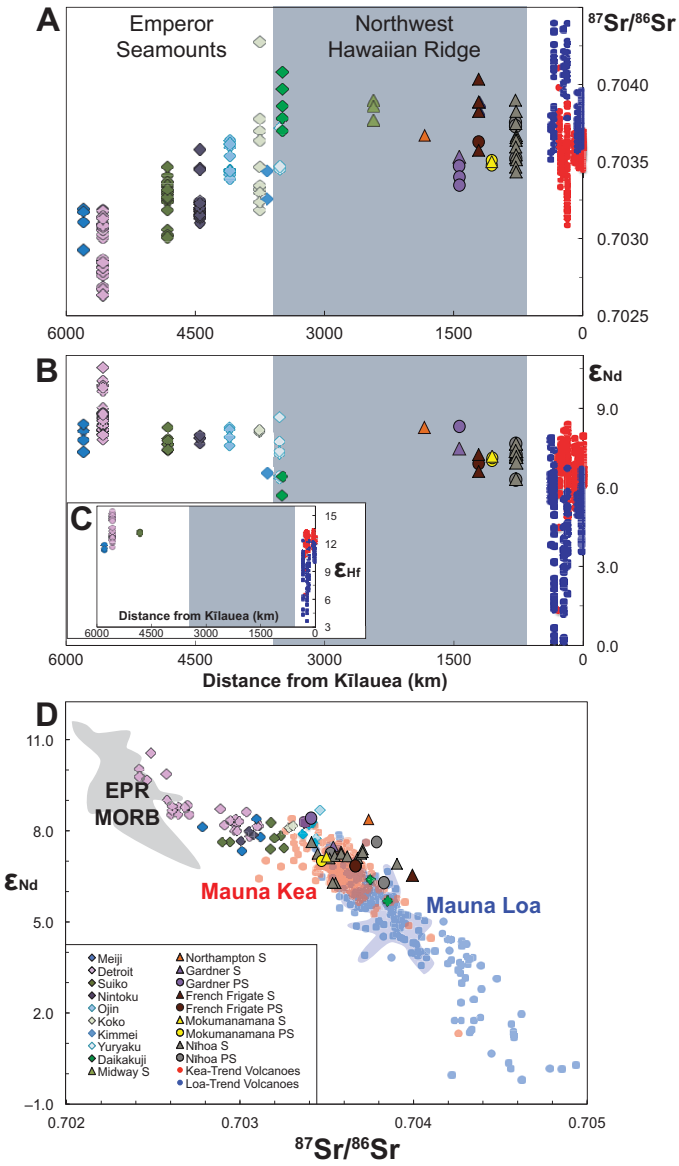

Figure 8. Plots of isotopic variation versus distance along the Hawaiian-Emperor Chain. (A) Sr. (B) Nd. (C) Hf. The Emperor Seamount samples are from shield and post-shield stages (both shown as diamonds; see Appendix Table A1). The Hawaiian Islands samples (younger than 5 Ma) are only from the shield stage and are subdivided into Loa (blue symbols) and Kea (red symbols) trends (after Weis et al., 2011). The Northwest Hawaiian Ridge samples are subdivided into shield (triangle) and post-shield (circles) stages. The gray box defines the Northwest Hawaiian Ridge section of the chain. (D) Plot of ε_{Nd} versus $^{87}Sr/^{86}Sr$. Fields are shown for lavas from Mauna Kea and Mauna Loa volcanoes, and East Pacific Rise mid-oceanic ridge basalt (EPR MORB). Isotopic data for the Hawaiian Islands is from the compilation of Tanaka et al. (2008). Sources for the Emperor Seamount and Hawaiian Ridge data are given in Appendix Table A1. East Pacific Rise MORB data were downloaded from the PetDB website (Integrated Earth Data Applications Petrological Database; http://www.earthchem.org/petdb) site on 8 November 2012, using the filter of fresh glasses only. All values were renormalized to the same isotopic standard values following the procedures described in text.

(e.g., Macdonald et al., 1983), despite the dramatic variation in the size of the Northwest Hawaiian Ridge volcanoes (<1–54 × 10^3 km^3; Bargar and Jackson, 1974).

The scarcity of rejuvenated lavas among the Northwest Hawaiian Ridge volcanoes is surprising. Only 4 of 27 sampled seamounts (~15% of the sampled Northwest Hawaiian Ridge volcanoes) are reported to have rejuvenated lavas (Clague and Dalrymple, 1989). These four seamounts span nearly the full length of the Northwest Hawaiian Ridge (Mokumanamana to Colahan; Fig. 1). In the absence of reliable ages for most of the Northwest Hawaiian Ridge, the identification of rejuvenated lavas is usually based on petrography (presence of characteristic minerals such as feldspathoids and/or strongly colored clinopyroxene; e.g., Winchell, 1947) and geochemistry (strongly alkalic basalts and isotopically depleted compositions). In the Hawaiian Islands, rejuvenated lavas are present on ~50% of the volcanoes (Sherrod et al., 2007). Why have rejuvenated lavas been recovered from so few Northwest Hawaiian Ridge seamounts? Perhaps the rejuvenated lavas are buried under carbonate reefs on the summits of the seamounts and by sediment on their flanks, or have been eroded. Alternatively, the higher occurrence of rejuvenated volcanism for the Hawaiian Islands, especially on and around the northern islands (Garcia et al., 2008), may be related to the sudden increase in magma flux just before the islands (Fig. 2). More multibeam surveys and sampling are needed along the Northwest Hawaiian Ridge to search for products of rejuvenated volcanism to ensure that the rarity of these lavas is not simply a sampling issue in the current database. It is interesting to note that rejuvenated volcanism was not found on the Louisville Seamounts (Vanderkluysen et al., 2014).

Age of the Hawaiian-Emperor Bend?

The bend, the most distinctive feature of the Hawaiian-Emperor Chain, has been the focus of several geochronologic campaigns (Dalrymple and Clague, 1976; Clague and Dalrymple, 1987; Sharp and Clague, 2006; O'Connor et al., 2013). For decades, the accepted age of the Hawaiian-Emperor Bend was ca. 43 Ma (e.g., Clague and Dalrymple, 1987). However, this age estimate was found to be erroneous after new $^{40}Ar/^{39}Ar$ ages were determined (Sharp and Clague, 2006). These results as well as those of O'Connor et al. (2013) call into question most of the early published ages on the Northwest Hawaiian Ridge. Sharp and Clague (2006) suggested that initiation of the Hawaiian-Emperor Bend occurred near Kimmei Seamount at 50.0 ± 0.09 Ma. This age is based on an interpolation for the age of the Kimmei shield stage by fitting a linear trend to dated shield stage lavas from adjacent seamounts (Koko's northern eruptive enter, Daikakuji and Abbott seamounts). The recent adjusted linear fit model of O'Connor et al. (2013) also predicts a 50 Ma age for Kimmei. However, O'Connor et al. (2013) suggested that the arcuate bend in the Hawaiian-Emperor Chain occurred at Daikakuji and Yuryaku seamounts at 47.5 Ma. We prefer the approach used by Wessel et al. (2006) to estimate the location

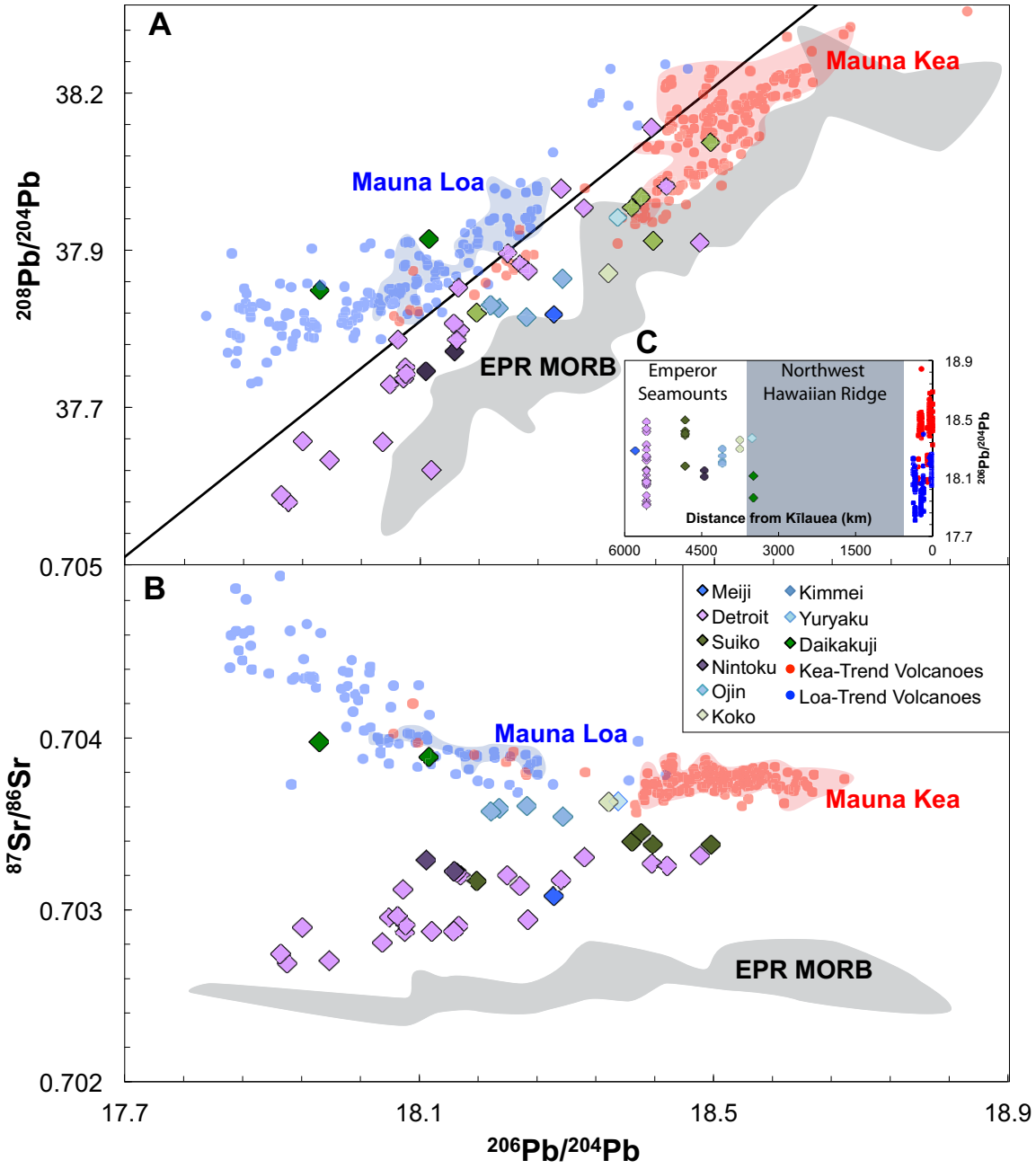

Figure 9. Pb isotopic variation of the Hawaiian-Emperor Chain. (A) Plot of $^{208}Pb/^{204}Pb$ versus $^{206}Pb/^{204}Pb$. The black line represents the boundary between Loa-trend and Kea-trend volcanoes as defined by Abouchami et al. (2005). (B) $^{87}Sr/^{86}Sr$ versus $^{206}Pb/^{204}Pb$ plot. Daikakuji is the only Northwest Hawaiian Ridge volcano for which Pb isotopic data are available. (C) Plot of $^{206}Pb/^{204}Pb$ versus distance from Kīlauea. In all diagrams, fields shown are for Mauna Kea and Mauna Loa volcanoes, and EPR MORB. Data sources and data treatment are as in Figure 8.

of the bend; within a 95% confidence, they placed the bend at 33.1°N and 171.9°E, which is at Toba (Fig. 1), an undated seamount located 40 km south of Kimmei Seamount and ~90 km northwest of Yuryaku Seamount.

An age for Kimmei of 47.9 ± 0.2 Ma is based on plagioclase from a post-shield lava (Sharp and Clague, 2006). Therefore, the shield stage of Kimmei likely occurred between 49 and 48 Ma. Ages from Yuryaku Seamount are highly variable, but the oldest shield stage sample has a $^{40}Ar/^{39}Ar$ age of 47.4 ± 0.4 Ma (Fig. 3). Initiation of the Hawaiian-Emperor Bend must be younger than the shield stage of Kimmei, but older than the ages from Yuryaku. Thus, initiation of the Hawaiian-Emperor Bend

probably occurred at 49–48 Ma, which is several million years younger than the onset of subduction along the western edge of the Pacific plate as inferred from U-Pb zircon ages from forearc gabbros in the Izu-Bonin-Mariana (51.7 ± 0.6 Ma; Ishizuka et al., 2011) and Tonga arc systems (51.2 ± 0.8 Ma; Meffre et al., 2012). This contradicts the findings of several recent studies (e.g., Sharp and Clague, 2006; Reagan et al., 2010; Ishizuka et al., 2011; O'Connor et al., 2013) that supported a causal link between the major shift in Pacific plate motion associated with initiation of subduction in the western Pacific and formation of the Hawaiian-Emperor Bend. A 49–48 Ma age for initiation of the bend does not preclude a link between the two events, but rather suggests that they were not synchronous.

It is important to note that the older bend in the Louisville Ridge at 169°W is estimated to have been completed by ca. 51–50 Ma, and this likely represents a minimum age for that bend (Koppers et al., 2004, 2011). Thus, it appears the age of the older Louisville Ridge bend more closely coincides with western Pacific subduction initiation, and both preceded the bend in the Hawaiian-Emperor Chain.

Source Variation for the Hawaiian-Emperor Chain

The lack of modern high-precision isotopic data from rocks from the Northwest Hawaiian Ridge precludes a detailed assessment of the geochemical evolution of the Hawaiian mantle plume for the 42–6 Ma period (Fig. 8). Comparison of isotopic signatures for rocks from the Emperor Seamounts and Hawaiian Islands provides some limited information. Sr isotope ratios increase almost continuously in the older stages of the Emperor Seamounts with decreasing age, but are relatively homogeneous and lacking any trend along the Northwest Hawaiian Ridge (Fig. 8). This suggests that the mechanism causing the depleted Sr isotopic signatures was not affecting the Hawaiian mantle plume by about 50 Ma, consistent with increasing distance of the Hawaiian plume from a spreading ridge with decreasing age along the chain (Huang et al., 2005; Regelous et al., 2003; Keller et al., 2000). However, the presence of depleted isotopic ratios along the entire Hawaiian-Emperor Chain suggests that the source of this signature is an intrinsic and persistent component of the Hawaiian mantle plume, which confirms the interpretation of Frey et al. (2005) and others.

Isotopic data can be used to determine the spatial and temporal extent of different source components in the Hawaiian mantle plume. These aspects of plume history are particularly important for resolving the controversy regarding the origin of the distinctive Loa geochemical source component observed in the young Hawaiian lavas (younger than 5 Ma). The Hawaiian Islands have been classified into two geochemical trends, termed the Loa and the Kea trends, based on different major and trace element chemistry, isotopic signature, and geographical location (Jackson et al., 1972; Tatsumoto, 1978; Abouchami et al., 2005; Weis et al., 2011). Kea-like compositions are observed in both Emperor Seamount and Hawaiian Island lavas (e.g., Tanaka et al., 2008), whereas Loa-like compositions were previously identified only in volcanoes younger than 5 Ma (e.g., Garcia et al., 2010; Greene et al., 2010). Lavas with unradiogenic Pb, low ε_{Nd}, and high $^{87}Sr/^{86}Sr$ isotopes have been reported from Daikakuji Seamount (Fig. 9), suggesting that the Loa component may have appeared in the Hawaiian plume as early as ca. 47 Ma, near the bend in the Hawaiian-Emperor Chain. Careful analysis of leached samples is critical to confirm this observation and to evaluate the extent of the Loa component among Northwest Hawaiian Ridge volcanoes because the presence of this source component has important implications for the magma flux variations for the Hawaiian Ridge (see following).

Magma Flux Variations along the Hawaiian Ridge

The magmatic productivity of mantle plumes is highly variable on local and regional scales (e.g., Vogt, 1972; White, 1993). Along the Hawaiian-Emperor Chain, the local variations are evident in the size differences between adjacent volcanoes (e.g., west Maui and Haleakalā, 9 versus 70×10^3 km^3; Robinson and Eakins, 2006). To evaluate regional magma flux variations, 10 m.y. time segments of the Hawaiian-Emperor Chain were examined for the volume calculations to minimize the local variations (e.g., White, 1993). Previous studies have used a variety of approaches including bathymetry (with or without gravity corrections) and various fluid dynamic models to determine the regional variations in the magmatic flux along the Hawaiian-Emperor Chain (e.g., Bargar and Jackson, 1974; Sleep, 1990; White, 1993; Ribe and Christensen, 1994; Van Ark and Lin, 2004; Vidal and Bonneville, 2004). Despite the different approaches, some consistent trends emerge in the magma flux estimates for the Hawaiian-Emperor Chain. (1) The Emperor Seamounts had relatively low magma flux with moderate variations (2 ± 1 m^3 s^{-1}; Fig. 2). (2) The older section of the Northwest Hawaiian Ridge (older than 30 Ma) had low to very low magma output (1–2 m^3 s^{-1}) with the lowest flux ca. 35 Ma (Fig. 2). (3) The younger section of the Northwest Hawaiian Ridge and the Hawaiian Islands had an order of magnitude increase in magma output to values >20 m^3 s^{-1}, with a maximum at the southern end of the islands and a major high for Gardner volcano (Fig. 2). These overall features are robust and independent of the compensation model used (Vidal and Bonneville, 2004). In the following paragraphs, we review and evaluate some of the previously proposed explanations for the flux variations.

The processes invoked to explain magma flux variations for the Hawaiian-Emperor Chain can be subdivided into two groups, lithosphere related and plume related. The lithosphere-related processes include the following: (1) Faster plate motion causes higher output rates (Vogt, 1972). Although there is a crude overall variation in the output rate of the Hawaiian-Emperor Chain with estimated plate velocity, the Louisville Ridge shows an opposite trend (Koppers et al., 2011), so this idea is not valid for hotspot trails in general. (2) Variations in lithosphere thickness (White, 1993). Thinner, warmer lithosphere allows greater

extents of melting (Regelous et al., 2003). Along the Hawaiian-Emperor Chain, there is no clear correlation between magma production rate and lithosphere thickness (White, 1993) or with the presence of fracture zones (Epp, 1984). The marked increase in lithosphere thickness from north to south under the Emperor Seamounts is not correlated with higher magma production (White, 1993). (3) Changes in plate stresses resulting from reconfigurations of plate motion (e.g., Sager and Keating, 1984; Koppers and Staudigel, 2005; Wessel and Kroenke, 2009). This model attributes variations in magma flux to fluctuations in the lithosphere's state of stress driven by changes in the absolute motion of the Pacific plate. Depending on the direction of these changes and location on the plate, a region may undergo an increase in tensional (more melting) or compressional stresses (less melting), which modulates the amount of melt reaching the surface (Hieronymus and Bercovici, 1999). At present, we are not able to evaluate the viability of this model.

Potential plume-related causes for the variations in magma flux include the following. (1) Southward migration of the Hawaiian hotspot (Tarduno et al., 2003). This migration stopped at or before the bend in the Hawaiian-Emperor Chain, so hotspot drift is unable to explain the magma flux variation for the past 50 m.y. (2) Periodic oscillation in the plume conduit diameter (e.g., Ito, 2001). This model suggests that plumes may have solitary waves formed at boundary layers that cause perturbations in magma flux (the plume conduit swells or contracts with more of less plume mass; e.g., Sleep, 1992). Solitary waves have been invoked to explain V-shaped ridges along the Mid-Atlantic Ridge (Iceland and Azores; Ito, 2001; Escartin et al., 2001). White (1993) reasoned that the effects of solitary waves in the mantle are smoothed by using 10 m.y. time slices for volume calculations. Thus, the overall increase in melt production for the Northwest Hawaiian Ridge is probably not be related to changes in the plume conduit diameter. (3) Changes in melting conditions (temperature and/or pressure; Vogt, 1972; Sleep, 1990; Jull and McKenzie, 1996). For example, the order of magnitude increase in magma output over the past 30 m.y. along the Hawaiian Ridge was estimated to require an ~150 °C temperature increase, assuming that other parameters were constant (Vogt, 1972). Currently, there are no geochemical data to evaluate whether there was a decrease in pressure or increase in temperature of melting. (4) Alternatively, a marked change in source fertility (related to rock type, pyroxenite versus peridotite, and/or previous melting history; Hofmann, 1988; Sobolev et al., 2007; Lee et al., 2009) might be responsible for the remarkable increase in magma output of the Hawaiian plume. Lavas with Loa-type isotopic compositions were reported from Daikakuji Seamount, just south of the bend in the Hawaiian-Emperor Chain (Fig. 9). The Loa geochemical signature is thought to be related to melting of a pyroxenite rather than a peridotite source (e.g., Hauri, 1996). Pyroxenite melts at a lower temperature than peridotite, so its presence in the source of Northwest Hawaiian Ridge lavas might correlate with higher magma flux. However, the Daikakuji area of the ridge was not a region of high melt output (White, 1993).

To assess the possible source composition of lavas from elsewhere along the Northwest Hawaiian Ridge where there are no Pb isotope data, we examined ratios of major elements that are thought to be distinctive of the source component in Hawaiian Island tholeiitic lavas and that are insensitive to olivine fractionation (Na_2O/TiO_2 and CaO/Al_2O_3). Jackson et al. (2012) found that the Loa-type source component (best shown for Ko'olau lavas) higher Na_2O/TiO_2 and lower CaO/Al_2O_3 than Kea-type lavas (Jackson et al., 2012). If we consider only tholeiitic Northwest Hawaiian Ridge lavas with MgO > 8 wt% that contain only modal olivine (11 samples from 6 volcanoes), there is an overall increase in the CaO/Al_2O_3 ratio from Nīhoa to East Northampton volcano (0.69–0.94, but with considerable local variation between adjacent volcanoes, 0.81–0.94). Only the transitional lava from West Nīhoa overlaps in CaO/Al_2O_3 with the Makapu'u component of Ko'olau (0.69 versus <0.73). There is no regional pattern in Na_2O/TiO_2 in Northwest Hawaiian Ridge and none have ratios as high as those of Makapu'u component (>1.1; Table 3). Overall, the major element chemistry of most Northwest Hawaiian Ridge lavas are Kea-like. With the current limited data set for Northwest Hawaiian Ridge, the question of when the Loa component arrived and what effect it had on melt flux is unresolved. Evaluation of the longevity of the Loa component in the source for Hawaiian magmas requires new high-precision isotopic data and more whole-rock chemistry data from lavas of the Northwest Hawaiian Ridge.

We have shown that some of the proposed mechanisms to explain the dramatic increase in melt flux along the Hawaiian Ridge are probably not valid (e.g., variations in plate thickness, plate velocity, and plume conduit size), whereas others (changes melting conditions and fertility of the source) need additional evaluation through new geochemical, isotopic, and modeling studies.

SUMMARY

We have presented a new bathymetric compilation of the Northwest Hawaiian Ridge, and new petrographic and XRF data for lavas recently collected using the *Pisces V* submersible and other samples from 12 volcanoes spanning ~1900 km of the Northwest Hawaiian Ridge. In addition, the current state of knowledge on the age and isotopic variations along the Northwest Hawaiian Ridge has been reviewed. These new results and analysis show the following:

1. Determining the number seamounts along the Northwest Hawaiian Ridge is complicated by the incomplete bathymetric data set and the presence of Cretaceous seamounts along and near the ridge. We recognized 51 volcanoes along the Northwest Hawaiian Ridge based on new and previous sampling and/or the location of the seamount within the trend of the ridge. Lavas have been recovered from 27 of the 51 volcanoes; more volcanoes may be present within the Northwest Hawaiian Ridge, as suggested by others, although additional surveying and sampling are needed to confirm their presence.

2. The rock types along the Northwest Hawaiian Ridge are the same as observed on the Hawaiian Islands with tholeiitic shield and alkalic post-shield lavas found on many of the sampled volcanoes. However, examples of rejuvenated volcanism are much less common among the samples taken along the Northwest Hawaiian Ridge than on and around the Hawaiian Islands (15% versus 50% of the volcanoes). This may be related to extensive development of carbonate reefs on the Northwest Hawaiian Ridge volcanoes obscuring their presence, their removal via erosion, or the fact that the limited sampling to date has not encountered them. Alternatively, the scarcity of rejuvenated volcanism could be a consequence of plume processes related to less extensive melt flux for the Northwest Hawaiian Ridge versus the Hawaiian Islands.

3. The absolute age and duration of volcanism for individual volcanoes are poorly known for most of the Northwest Hawaiian Ridge. Few samples from these volcanoes have been dated by modern $^{40}Ar/^{39}Ar$ methods, and those that have been analyzed with modern methods are concentrated near the bend in Hawaiian-Emperor Chain. Thus, the rate of Pacific plate motion during much of the late Cenozoic is not well constrained by the existing ages for the Northwest Hawaiian Ridge.

4. The initiation age of the bend in the Hawaiian-Emperor Chain is ca. 49–48 Ma. This age is slightly younger than previously reported (ca. 50 Ma) and the age for the onset of island arc volcanism in the western Pacific (52–51 Ma). Our interpretation of a younger age for initiation of the bend does not preclude a link between the start of arc volcanism and the change in direction of the Pacific plate (as reflected by the kink in the Hawaiian-Emperor Chain) but it indicates that they were not synchronous.

5. The Loa-trends source component was found in the isotopic data for two transitional lavas from Daikakuji Seamount near the bend in the Hawaiian-Emperor Chain. Otherwise, all the other isotopic data, which are extremely limited, especially for Pb and whole-rock XRF data for Northwest Hawaiian Ridge lavas indicate only Kea trend source compositions.

6. The well-known dramatic increase in melt flux for the Hawaiian Ridge is probably not related to some of the previously proposed mechanisms (variations in plate thickness, plate velocity, and plume conduit size). Melt flux variations may be related to changes in melting conditions, source fertility, or plate stress, although more work is needed to evaluate these alternatives.

ACKNOWLEDGMENTS

We thank Alexandra Hangsterfer (Scripps Institution of Oceanography Geological Collections Manager) for invaluable help in locating critical samples from the University of California at San Diego Scripps collection, Adonara Mucek for organizing the University of Hawai‘i rock collection, and Kim Rottas and Zara Huntley for X-ray fluorescence sample preparation. Reviews by Robert Duncan and J.M. Rhodes improved the manuscript. This research was supported by National Science Foundation grant EAR-1219955 to Garcia, a Natural Sciences and Engineering Research Council of Canada Discovery Grant to Weis, and a National Oceanic and Atmospheric Administration Office of Ocean Exploration and Research and National Marine Sanctuaries grant to Smith. Lauren Harrison benefited from a University of British Columbia four year fellowship. This paper is University of Hawai‘i SOEST contribution 8969.

APPENDIX. Sr-Hf-Nd-Pb ISOTOPES: EMPEROR-HAWAIIAN CHAIN

TABLE A1. COMPILED Sr-Hf-Nd-Pb ISOTOPES FOR THE EMPEROR SEAMOUNTS AND NORTHWEST HAWAIIAN RIDGE

Volcano name	Volcanic stage	Distance from Kīlauea (km)	Inferred age (Ma)	Sample number	$^{206}Pb/^{204}Pb$	$^{207}Pb/^{204}Pb$	$^{208}Pb/^{204}Pb$	$^{208}Pb^*/^{206}Pb^*$	$^{87}Sr/^{86}Sr$	$^{143}Nd/^{144}Nd$	ε_{Nd}	$^{176}Hf/^{177}Hf$	ε_{Hf}	Reference
Emperor Seamount Chain														
Meiji	S	5800	85	192-6-2	18.2828	15.4343	37.8084	0.9283	0.702972	0.512956	8.34			Keller et al., 2000
Meiji	S	5800	85	19-1	17.8050	15.4419	37.8862	0.9897	0.702927	0.512946	8.14	0.283050	9.83	Regelous et al., 2003; Frey et al., 2005
Meiji	S	5800	85	19-2	17.8820	15.4280	37.7596	0.9660	0.703109	0.512905	7.34	0.283051	9.87	Regelous et al., 2003; Frey et al., 2005
Meiji	S	5800	85	19-3	17.8479	15.4308	37.8023	0.9749	0.703194	0.512929	7.81	0.283036	9.34	Regelous et al., 2003; Frey et al., 2005
Meiji	S	5800	85	19-4	17.5257	15.4161	37.8555	1.0196	0.703175	0.512959	8.40	0.283040	9.48	Regelous et al., 2003; Frey et al., 2005
Suiko	S	4827	64.7	433-31-1	18.3978	15.4563	37.9625	0.9335	0.703257	0.512976	8.22			Keller et al., 2000
Detroit	S	5580	80	883-1-3	17.9417	15.4263	37.6063	0.9416	0.702808	0.512969	8.47			Keller et al., 2000
Detroit	S	5580	80	883-2-3	18.1167	15.4373	37.5603	0.9177	0.702788	0.512988	8.84			Keller et al., 2000
Detroit	S	5580	81.2	884-6-3	18.0507	15.4163	37.6053	0.9297	0.702730	0.513050	10.08			Keller et al., 2000
Detroit	S	5580	81.2	884-10-4	17.9217	15.4063	37.5093	0.9325	0.702620	0.513017	9.43			Keller et al., 2000
Detroit	PS	5580	81	145-1	18.0812	15.4258	37.7237	0.9400	0.702784	0.512972	6.52	0.283087	11.14	Regelous et al., 2003; Frey et al., 2005
Detroit	PS	5580	81	145-2	17.8099	15.4270	37.7582	0.9740	0.702786	0.512979	6.65	0.283076	10.75	Regelous et al., 2003; Frey et al., 2005
Detroit	PS	5580	81	145-3	18.1528	15.4440	37.8505	0.9467	0.702816	0.512985	6.77	0.283079	10.86	Regelous et al., 2003; Frey et al., 2005
Detroit	PS	5580	81	145-4					0.702762	0.512996	6.98	0.283088	11.18	Regelous et al., 2003; Frey et al., 2005
Detroit	S	5580	81	145-7					0.702635	0.513049	8.02	0.283135	12.84	Regelous et al., 2003; Frey et al., 2005
Detroit	S	5580	81	145-8					0.702759	0.513040	7.84	0.283130	12.66	Regelous et al., 2003; Frey et al., 2005
Detroit	S	5580	81	145-9					0.702688	0.513075	8.52	0.283149	13.33	Regelous et al., 2003; Frey et al., 2005
Detroit	S	5580	81	145-10	17.9120	15.4189	37.5213	0.9350	0.702670	0.513030	7.65	0.283139	12.98	Regelous et al., 2003; Frey et al., 2005
Detroit	S	5580	81	145-11	17.9777	15.4250	37.5761	0.9342	0.702635	0.513036	7.76	0.283156	13.58	Regelous et al., 2003
Detroit	TB	5580	76	1203A 17 R4W 43-47	18.4808	15.4643	37.9222	0.9207	0.703187	0.512955	8.09	0.283078	10.82	Huang et al., 2005; Frey et al., 2005
Detroit	TB	5580	76	1203A 20 R3W 10-14	18.3238	15.4883	37.9772	0.9428	0.703178	0.512954	8.07	0.283075	10.72	Huang et al., 2005; Frey et al., 2005
Detroit	TB	5580	76	1203A 31 R1W 46-50	18.2198	15.4743	37.9052	0.9457	0.703080	0.512966	8.31	0.283102	11.67	Huang et al., 2005; Frey et al., 2005
Detroit	TB	5580	76	1203A 32 R4W 76-80	18.1558	15.4603	37.7832	0.9388	0.703080	0.512952	8.03	0.283080	10.89	Huang et al., 2005; Frey et al., 2005
Detroit	TB	5580	76	1203A 38 R1W 123-126	18.0787	15.4523	37.7061	0.9383	0.703008	0.512984	8.66	0.283109	11.92	Huang et al., 2005; Frey et al., 2005
Detroit	TB	5580	76	1203A 49 R3W 50-54	18.2368	15.4693	37.8882	0.9420	0.703027	0.512957	8.13	0.283098	11.53	Huang et al., 2005; Frey et al., 2005
Detroit	AB	5580	76	1203A 54 R4W 74-78	18.4158	15.4793	38.1052	0.9474	0.703143	0.512938	7.76	0.283073	10.64	Huang et al., 2005; Frey et al., 2005
Detroit	TB	5580	76	1203A 59 R2W 69-73	18.1508	15.4673	37.7672	0.9375	0.703094	0.512962	8.23	0.283109	11.92	Huang et al., 2005; Frey et al., 2005
Detroit	AB	5580	76	1203 63 R4W 19-22	18.2928	15.4553	38.0082	0.9495	0.703056	0.512965	8.29	0.283064	10.33	Huang et al., 2005; Frey et al., 2005

(*Continued*)

TABLE A1. COMPILED Sr-Hf-Nd-Pb ISOTOPES FOR THE EMPEROR SEAMOUNTS AND NORTHWEST HAWAIIAN RIDGE (*Continued*)

Volcano name	Volcanic stage	Distance from Kīlauea (km)	Inferred age (Ma)	Sample number	$^{206}Pb/^{204}Pb$	$^{207}Pb/^{204}Pb$	$^{208}Pb/^{204}Pb$	$^{208}Pb^*/^{206}Pb^*$	$^{87}Sr/^{86}Sr$	$^{143}Nd/^{144}Nd$	ε_{Nd}	$^{176}Hf/^{177}Hf$	ε_{Hf}	Reference
Emperor Seamount Chain (*Continued*)														
Detroit	AB	5580	76	1203A 65 R4W 9-13	18.1868	15.4763	38.3253	0.9966	0.703078	0.512948	7.96	0.283051	9.87	Huang et al., 2005; Frey et al., 2005
Detroit	AB	5580	76	1203A 66 R2W 8-10	18.2448	15.4683	38.1302	0.9683	0.703089	0.512947	7.94	0.283079	10.86	Huang et al., 2005; Frey et al., 2005
Detroit	TB	5580	76	1203A 68 R4W 40-43	18.4358	15.5053	38.0112	0.9350	0.703129	0.512978	8.54	0.283067	10.43	Huang et al., 2005; Frey et al., 2005
Detroit	AB	5580	76	1204A R2W 108-112	18.0597	15.4503	37.6971	0.9393	0.702859	0.512990	8.78	0.283144	13.16	Huang et al., 2005; Frey et al., 2005
Detroit	AB	5580	76	1204B 3 R2W 41-44	18.1467	15.4473	37.7932	0.9409	0.702788	0.512988	8.74	0.283138	12.94	Huang et al., 2005; Frey et al., 2005
Detroit	AB	5580	76	1204B 7 R3W 68-72	18.0817	15.4673	37.7141	0.9388	0.702820	0.512974	8.46	0.283147	13.26	Huang et al., 2005; Frey et al., 2005
Detroit	AB	5580	76	1204B 10 R4W 43-47	18.0707	15.4553	37.7682	0.9462	0.702866	0.512974	8.46	0.283136	12.87	Huang et al., 2005; Frey et al., 2005
Detroit	AB	5580	76	1204B 17 R1W 107-110	18.2478	15.4473	37.8772	0.9396	0.702848	0.512986	8.70	0.283131	12.70	Huang et al., 2005; Frey et al., 2005
Suiko	PS	4827	64.7	55-9	18.1790	15.4483	37.8096	0.9393	0.703056	0.512949	7.69			Regelous et al., 2003
Suiko	PS	4827	64.7	55-10					0.703021	0.512948	7.67			Regelous et al., 2003
Suiko	S	4827	64.7	55-12	18.4184	15.4547	37.9235	0.9271	0.703243	0.512982	8.34			Regelous et al., 2003
Suiko	S	4827	64.7	55-13					0.703287	0.512960	7.91			Regelous et al., 2003
Suiko	S	4827	64.7	55-14	18.3893	15.4592	37.9765	0.9359	0.703259	0.512956	7.83			Regelous et al., 2003
Suiko	S	4827	64.7	55-15	18.4967	15.4697	38.0806	0.9363	0.703241	0.512937	7.46			Regelous et al., 2003
Suiko	S	4827	64.7	55-16	18.4023	15.4584	37.9927	0.9364	0.703302	0.512939	7.50			Regelous et al., 2003
Suiko	S	4827	64.7	433-31-1	18.3978	15.4563	37.9625	0.9335	0.703257	0.512976	8.22			Keller et al., 2000
Suiko	TB	4827	64.7	DSDP 55-433C-13-2:55-56								0.283100	11.60	Frey et al., 2005
Suiko	TB	4827	64.7	DSDP 55-433C-19-5:57-65								0.283105	11.78	Frey et al., 2005
Suiko	TB	4827	64.7	DSDP 55-433C-39-5:87-94								0.283097	11.49	Frey et al., 2005
Suiko	TB	4827	64.7	DSDP 55-433C-42-1:56-63								0.283101	11.63	Frey et al., 2005
Suiko	PS	4827	64.7	433A-20-1, 30-36					0.703007					Lanphere et al., 1980
Suiko	PS	4827	64.7	433A-21-4, 129-138					0.703187					Lanphere et al., 1980
Suiko	PS	4827	64.7	433B-5-2, 61-68					0.703337					Lanphere et al., 1980
Suiko	PS	4827	64.7	433C-4-1, 25-28					0.703407					Lanphere et al., 1980
Suiko	S	4827	64.7	433C-15-6, 16-31					0.703267					Lanphere et al., 1980
Suiko	S	4827	64.7	433C-17-1, 69-82					0.703367					Lanphere et al., 1980
Suiko	S	4827	64.7	433C-28-2, 73-80					0.703347					Lanphere et al., 1980
Suiko	S	4827	64.7	433C-29-2, 94-100					0.703467					Lanphere et al., 1980
Suiko	S	4827	64.7	433C-31-1, 28-34					0.703317					Lanphere et al., 1980
Nintoku	PS	4452	56.2	55-5	18.1489	15.4539	37.7472	0.9355	0.703103	0.512959	7.67			Regelous et al., 2003
Nintoku	PS	4452	56.2	55-6	18.1106	15.4461	37.7157	0.9359	0.703162	0.512969	7.87			Regelous et al., 2003
Nintoku	PS	4452	56.2	55-8					0.703140	0.512975	7.99			Regelous et al., 2003
Nintoku	PS	4452	56	5R-2, 21-25					0.703141	0.512927	7.04			Schafer et al., 2005
Nintoku	PS	4452	56	5R-2, 90-94					0.703221	0.512989	8.25			Schafer et al., 2005
Nintoku	PS	4452	56	5R2, 96-100					0.703131	0.512941	7.32			Schafer et al., 2005
Nintoku	PS	4452	56	6R-2, 8-12					0.703157	0.512948	7.45			Schafer et al., 2005
Nintoku	PS	4452	56	10R-2, 0-5					0.703142	0.512968	7.84			Schafer et al., 2005

(*Continued*)

TABLE A1. COMPILED Sr-Hf-Nd-Pb ISOTOPES FOR THE EMPEROR SEAMOUNTS AND NORTHWEST HAWAIIAN RIDGE (*Continued*)

Volcano name	Volcanic stage	Distance from Kīlauea (km)	Inferred age (Ma)	Sample number	$^{206}Pb/^{204}Pb$	$^{207}Pb/^{204}Pb$	$^{208}Pb/^{204}Pb$	$^{208}Pb^*/^{206}Pb^*$	$^{87}Sr/^{86}Sr$	$^{143}Nd/^{144}Nd$	ε_{Nd}	$^{176}Hf/^{177}Hf$	ε_{Hf}	Reference
Emperor Seamount Chain (*Continued*)														
Nintoku	PS	4452	56	15R-3, 10-12					0.703175	0.512951	7.51			Schafer et al., 2005
Nintoku	PS	4452	56	19R-1, 80-86					0.703175	0.512946	7.41			Schafer et al., 2005
Nintoku	PS	4452	56	20R-5, 67-72						0.512958	7.65			Schafer et al., 2005
Nintoku	PS	4452	56	21R-3, 71-76						0.512942	7.34			Schafer et al., 2005
Nintoku	PS	4452	56	23R-1, 85-90					0.703163	0.512970	7.88			Schafer et al., 2005
Nintoku	PS	4452	56	24R-1, 51-56					0.703162					Schafer et al., 2005
Nintoku	PS	4452	56	26R-2, 30-34					0.703181	0.512957	7.63			Schafer et al., 2005
Nintoku	PS	4452	56	27R-6, 124-129					0.703200	0.512944	7.38			Schafer et al., 2005
Nintoku	PS	4452	56	28R-3, 10-15					0.703203	0.512954	7.57			Schafer et al., 2005
Nintoku	PS	4452	56	29R-3, 18-23					0.703190					Schafer et al., 2005
Nintoku	PS	4452	56	29R-3, 92-95						0.512974	7.96			Schafer et al., 2005
Nintoku	PS	4452	56	29R-4, 117-121						0.512954	7.57			Schafer et al., 2005
Nintoku	PS	4452	56	32R-3, 17-22					0.703232	0.512957	7.63			Schafer et al., 2005
Nintoku	PS	4452	56	33R-2, 70-75					0.703191	0.512963	7.75			Schafer et al., 2005
Nintoku	PS	4452	56	34R-3, 79-84					0.703237	0.512958	7.65			Schafer et al., 2005
Nintoku	PS	4452	56	35R-3, 108-114					0.703201	0.512990	8.27			Schafer et al., 2005
Nintoku	PS	4452	56	37R-5, 38-42					0.703152	0.512967	7.82			Schafer et al., 2005
Nintoku	PS	4452	56	38R-1, 4-7					0.703154	0.512958	7.65			Schafer et al., 2005
Nintoku	PS	4452	56	41R-3, 18-23					0.703201					Schafer et al., 2005
Nintoku	PS	4452	56	42R-4, 12-16					0.703246	0.512955	7.59			Schafer et al., 2005
Nintoku	PS	4452	56	44R-2, 14-19					0.703228	0.512955	7.59			Schafer et al., 2005
Nintoku	PS	4452	56	44R-2, 116-121						0.512951	7.51			Schafer et al., 2005
Nintoku	PS	4452	56	44R-2, 115-118						0.512943	7.36			Schafer et al., 2005
Nintoku	PS	4452	56	432A-2-3, 37-43					0.703457					Lanphere et al., 1980
Nintoku	PS	4452	56	432A-3-2, 120-126					0.703447					Lanphere et al., 1980
Nintoku	PS	4452	56	432A-5-2, 57-66					0.703577					Lanphere et al., 1980
Ojin	PS	4102	55.2	55-1	18.2470	15.4580	37.8023	0.9314	0.703444	0.512956	7.59			Regelous et al., 2003
Ojin	PS	4102	55.2	55-2	18.2092	15.4557	37.8166	0.9369	0.703433	0.512991	8.27			Regelous et al., 2003
Ojin	PS	4102	55.2	55-3	18.1983	15.4587	37.8213	0.9386	0.703415	0.512987	8.19			Regelous et al., 2003
Ojin	S	4102	55.2	55-4	18.2961	15.4602	37.8633	0.9331	0.703389	0.512973	7.92			Regelous et al., 2003
Ojin	PS	4102	55.2	430A-4-2, 110-118					0.703637					Lanphere et al., 1980
Ojin	PS	4102	55.2	430A-5-1, 21-27					0.703597					Lanphere et al., 1980
Ojin	PS	4102	55.2	430A-6-3, 52-63					0.703537					Lanphere et al., 1980
Ojin	PS	4102	55.2	430A-6-4, 7-15					0.703617					Lanphere et al., 1980
Ojin	S	4102	55.2	430A-6-4, 140-150					0.703437					Lanphere et al., 1980
Koko	S	3758	48.1	A43D-a	18.3010	15.4620	37.8723	0.9335	0.703467	0.512992	8.11			Regelous et al., 2003
Koko	AB	3758	48.1	A44D-a	18.3581	15.4675	37.9321	0.9343	0.703323	0.512995	8.17			Regelous et al., 2003
Koko	AB	3758	48.1	A44D-b					0.703343	0.513003	8.33			Regelous et al., 2003
Koko	AB	3758	48.1	A7-43-13					0.703697					Lanphere et al., 1980
Koko	PS	3758	48.1	A7-43-33					0.704277					Lanphere et al., 1980
Koko	S	3758	48.1	A7-43-51					0.703297					Lanphere et al., 1980
Koko	PS	3758	48.1	A7-43-82					0.703187					Lanphere et al., 1980
Koko	PS	3758	48.1	A7-43-89					0.703237					Lanphere et al., 1980
Koko	S	3758	48.1	A7-44-5					0.703637					Lanphere et al., 1980
Koko	S	3758	48.1	A7-44-11					0.703777					Lanphere et al., 1980
Kimmei	PS	3668	39.9	A51D-a					0.703440	0.512947	7.03			Regelous et al., 2003
Kimmei	PS	3668	39.9	A7-52-50					0.703257					Lanphere et al., 1980

(*Continued*)

TABLE A1. COMPILED Sr-Hf-Nd-Pb ISOTOPES FOR THE EMPEROR SEAMOUNTS AND NORTHWEST HAWAIIAN RIDGE (*Continued*)

Volcano name	Volcanic stage	Distance from Kīlauea (km)	Inferred age (Ma)	Sample number	$^{206}Pb/^{204}Pb$	$^{207}Pb/^{204}Pb$	$^{208}Pb/^{204}Pb$	$^{208}Pb^*/^{206}Pb^*$	$^{87}Sr/^{86}Sr$	$^{143}Nd/^{144}Nd$	ε_{Nd}	$^{176}Hf/^{177}Hf$	ε_{Hf}	Reference
Northwest Hawaiian Ridge														
Yuryaku	PS	3541	43.4	A53D-b					0.703450	0.512979	7.74			Regelous et al., 2003
Yuryaku	S	3541	43.4	A53D-c	18.3714	15.4589	37.9608	0.9361	0.703468	0.513027	8.68			Regelous et al., 2003
Yuryaku	S	3541	43.4	A7-53-11					0.703717					Lanphere et al., 1980
Daikakuji	AB	3520	42.4	A55D-b	18.1144	15.4467	37.9263	0.9595	0.703701	0.512912	6.41			Regelous et al., 2003
Daikakuji	AB	3520	42.4	A55D-e	17.9654	15.4237	37.8450	0.9666	0.703780	0.512875	5.69			Regelous et al., 2003
Daikakuji	PS	3520	42.4	A7-55-25					0.703967					Lanphere et al., 1980
Daikakuji	S	3520	42.4	A7-55-29					0.703857					Lanphere et al., 1980
Daikakuji	PS	3520	42.4	A7-55-32					0.704077					Lanphere et al., 1980
East Northampton	S	1846		Northampton 5-4C					0.703669	0.513061	8.25			Basu and Faggart, 1996
Midway Island	PS	2447		R-1189					0.703897					Lanphere et al., 1980
Midway Island	PS	2447		R-1214					0.703767					Lanphere et al., 1980
Midway Island	PS	2447		R-1625					0.703857					Lanphere et al., 1980
Gardner	PS	1449		Gardner G7					0.703399	0.513063	8.29			Basu and Faggart, 1996
Gardner	S	1449		Gardner GP-6					0.703530	0.513021	7.47			Basu and Faggart, 1996
Gardner	PS	1449		72HIG-37-1					0.703347					Lanphere et al., 1980
Gardner	PS	1449		72HIG-37-2B					0.703467					Lanphere et al., 1980
French Frigate	S	1230		LPP 1N					0.703565	0.513012	7.30			Basu and Faggart, 1996
French Frigate	PS	1230		LPP 2S					0.703632	0.512989	6.85			Basu and Faggart, 1996
French Frigate	S	1230		LPP 3					0.703887	0.512976	6.59			Basu and Faggart, 1996
French Frigate	S	1230		LPP-W-20					0.704037					Lanphere et al., 1980
French Frigate	S	1230		LPP-W-30					0.703827					Lanphere et al., 1980
Mokumanamana	PS	1080		NEC 4					0.703509	0.513001	7.08			Basu and Faggart, 1996
Mokumanamana	S	1080		NEC 5					0.703500	0.513004	7.14			Basu and Faggart, 1996
Mokumanamana	PS	1080		NEC 8					0.703478	0.512997	7.00			Basu and Faggart, 1996
Nīhoa	S	794	7.2	NIH F2					0.703666	0.513016	7.37			Basu and Faggart, 1996
Nīhoa	S	794	7.2	NIH F5					0.703823	0.512992	6.91			Basu and Faggart, 1996
Nīhoa	S	794	7.2	NIH F5A					0.703657	0.513009	7.24			Basu and Faggart, 1996
Nīhoa	S	794	7.2	NIH F6					0.703667	0.513012	7.30			Basu and Faggart, 1996
Nīhoa	S	794	7.2	NIH F8					0.703535	0.513007	7.20			Basu and Faggart, 1996
Nīhoa	S	794	7.2	NIH F9					0.703595	0.513005	7.16			Basu and Faggart, 1996
Nīhoa	S	794	7.2	NIH W1					0.703641	0.513002	7.10			Basu and Faggart, 1996
Nīhoa	S	794	7.2	NIH W2					0.703431	0.513029	7.63			Basu and Faggart, 1996
Nīhoa	PS	794	7.2	NIH W4					0.703520	0.513011	7.28			Basu and Faggart, 1996
Nīhoa	S	794	7.2	NIH W7					0.703568	0.513009	7.24			Basu and Faggart, 1996
Nīhoa	S	794	7.2	NIH W10					0.703512	0.513002	7.10			Basu and Faggart, 1996
Nīhoa	S	794	7.2	NIH D1-1					0.703526	0.512961	6.30			Basu and Faggart, 1996
Nīhoa	S	794	7.2	NIH D1-2					0.703539	0.512960	6.28			Basu and Faggart, 1996
Nīhoa	PS	794	7.2	NIH D3					0.703762	0.512961	6.30			Basu and Faggart, 1996
Nīhoa	S	794	7.2	NIH D7					0.703459	0.513009	7.24			Basu and Faggart, 1996
Nīhoa	PS	794	7.2	NIH D9					0.703731	0.513029	7.63			Basu and Faggart, 1996
Nīhoa	S	794	7.2	8G104					0.703897					Lanphere et al., 1980
Nīhoa	S	794	7.2	8G141-2					0.703747					Lanphere et al., 1980
Ka'ula Rock	Rj	913		Kaula 79-KA-11					0.703745	0.512997	7.00			Basu and Faggart, 1996

Note: S—shield stage, PS—post-shield stage; Rj—rejuvenated stage; TB—tholeiitic basalt; AB—alkalic basalt. Data are adjusted for instrumental bias to $^{87}Sr/^{86}Sr = 0.710248$ for SRM987, $^{143}Nd/^{144}Nd = 0.511858$ for La Jolla, $^{176}Hf/^{177}Hf = 0.282160$ for JMC475. $^{206}Pb/^{204}Pb = 16.9405$, $^{207}Pb/^{204}Pb = 15.4963$, $^{208}Pb/^{204}Pb = 36.7219$ for SRM981. Present-day CHUR (chondritic uniform reservoir) values used here are 0.512638 for Nd and 0.282772 for Hf.

REFERENCES CITED

Abouchami, W., Hofmann, A.W., Galer, S.J.G., Frey, F.A., Eisele, J., and Feigenson, M., 2005, Lead isotopes reveal bilateral asymmetry and vertical continuity in the Hawaiian mantle plume: Nature, v. 434, p. 851–856, doi:10.1038/nature03402.

Althaus, T., Niedermann, S., and Erzinger, J., 2003, Noble gases in olivine phenocrysts from drill core samples of the Hawaii Scientific Drilling Project (HSDP) pilot and main holes (Mauna Loa and Mauna Kea, Hawaii): Geochemistry Geophysics Geosystems, v. 4, 8701, doi:10.1029/2001GC000275.

Bargar, K.E., and Jackson, E.D., 1974, Calculated volumes of individual shield volcanoes along the Hawaiian-Emperor Chain: U.S. Geological Survey Journal of Research, v. 2, p. 545–550.

Basu, A.R., and Faggart, B.E., 1996, Temporal isotopic variation in the Hawaiian mantle plume: The Lanai Anomaly, the Molokai Fracture Zone, and a seawater-altered lithospheric component in Hawaiian volcanism, *in* Basu, A., and Hart, S.R., eds., Earth Processes: Reading the Isotopic Code: American Geophysical Union Geophysical Monograph 95, p. 149–159, doi:10.1029/GM095p0149.

Becker, J.J., Sandwell, D.T., Smith, W.H.F., Braud, J., Binder, B., Depner, J., Fabre, D., Factor, J., Ingalls, S., Kim, S.-H., Ladner, R., Marks, K., Nelson, S., Pharaoh, A., Trimmer, R., Von Rosenberg, J., Wallace, G., and Weatherall, P., 2009, Global bathymetry and elevation data at 30 arc seconds resolution: SRTM30_PLUS: Marine Geodesy, v. 32, p. 355–371, doi:10.1080/01490410903297766.

Bianco, T., Ito, G., Becker, J., and Garcia, M.O., 2005, Secondary Hawaiian volcanism formed by flexural arch decompression: Geochemistry Geophysics Geosystems, v. 6, no. 8, Q08009, doi:10.1029/2005GC000945.

Blichert-Toft, J., Frey, F.A., and Albarède, F., 1999, Hf isotope evidence for pelagic sediments in the source of Hawaiian basalts: Science, v. 285, p. 879–882, doi:10.1126/science.285.5429.879.

Bryan, S.E., and Ernst, R.E., 2008, Revised definition of Large Igneous Provinces (LIPs): Earth-Science Reviews, v. 86, p. 175–202, doi:10.1016/j.earscirev.2007.08.008.

Clague, D.A., 1996, The growth and subsidence of the Hawaiian-Emperor volcanic chain, *in* Keast, A., and Miller, S.E., eds., The Origin and Evolution of Pacific Island Biotas, New Guinea to Eastern Polynesia: Patterns and Processes: Amsterdam, Academic Publishing, p. 35–50.

Clague, D.A., and Dalrymple, G.B., 1987, The Hawaiian-Emperor volcanic chain, *in* Decker, R. W., Wright, T.L., and Stauffer, P.H., eds., Volcanism in Hawaii: U.S. Geological Survey Professional Paper 1350, p. 5–54.

Clague, D.A., and Dalrymple, G.B., 1989, Tectonics, geochronology and origin of the Hawaiian-Emperor Chain, *in* Winterer, E.L., Hussong, D.M., and Decker, R.W., eds., The Eastern Pacific Ocean and Hawaii: Boulder, Colorado, Geological Society of America, Geology of North America, v. N, p. 187–217.

Clague, D.A., and Sherrod, D.R., 2014, Growth and degradation of Hawaiian volcanoes, *in* Poland, M.P., Takahashi, T.J. and Landowski, C.M., eds., Characteristics of Hawaiian Volcanoes: U.S. Geological Survey Professional Paper 1801, p. 97–146.

Clague, D.A., Dalrymple, G.B., and Moberly, R., 1975, Petrography and K-Ar ages of dredged volcanic rocks from the western Hawaiian Ridge and the southern Emperor Seamount Chain: Geological Society of America Bulletin, v. 86, p. 991–998, doi:10.1130/0016-7606(1975)86<991:PAKAOD>2.0.CO;2.

Coffin, M.F., and Eldholm, O., 1992, Volcanism and continental breakup: A global compilation of large igneous provinces, *in* Storey, B.C., Alabaster, T., and Pankhurst, R.J., eds., Magmatism and the Causes of Continental Break-up: Geological Society of London Special Publication 68, p. 17–30, doi:10.1144/GSL.SP.1992.068.01.02.

Coffin, M.F., and Eldholm, O., 1994, Large igneous provinces: Crustal structure, dimensions, and external consequences: Reviews of Geophysics, v. 32, p. 1–36, doi:10.1029/93RG02508.

Dalrymple, G.B., and Clague, D.A., 1976, Age of the Hawaiian-Emperor bend: Earth and Planetary Science Letters, v. 31, p. 313–329, doi:10.1016/0012-821X(76)90113-8.

Dalrymple, G.B., Lanphere, M.A., and Jackson, E.D., 1974, Contributions to the petrography and geochronology of volcanic rocks from the leeward Hawaiian Islands: Geological Society of America Bulletin, v. 85, p. 727–738, doi:10.1130/0016-7606(1974)85<727:CTTPAG>2.0.CO;2.

Dalrymple, G.B., Clague, D.A., and Lanphere, M.A., 1977, Revised age for Midway volcano, Hawaiian volcanic chain: Earth and Planetary Science Letters, v. 37, p. 107–116, doi:10.1016/0012-821X(77)90151-0.

Dalrymple, G.B., Clague, D.A., Garcia, M.O., and Bright, S.W., 1981, Petrology and K-Ar ages of dredged samples from Laysan Island and Northampton Bank volcanoes, Hawaiian evolution of the Hawaiian-Emperor chain: Geological Society of America Bulletin, v. 92, p. 884–933, doi:10.1130/GSAB-P2-92-884.

Dana, J.D., 1890, Characteristics of Volcanoes: With Contributions of Facts and Principles from the Hawaiian Islands: New York, London Dodd, Mead and Company, 399 p.

Duncan, R.A., and Clague, D.A., 1984, The earliest volcanism on the Hawaiian Ridge [abs]: Eos (Transactions, American Geophysical Union), v. 65, p. 1076.

Duncan, R.A., and Keller, R.A., 2004, Radiometric ages of basement rocks from the Emperor Seamounts, ODP Leg 197: Geochemistry Geophysics Geosystems, v. 5, Q08L03, doi:10.1029/2004GC000704.

Duncan, R.A., Tarduno, J.A., and Scholl, D.W., 2006, Leg 197 synthesis: Southward motion and geochemical variability of the Hawaiian hotspot, *in* Duncan, R.A., Tarduno, J.A., Davies, T.A., and Scholl, D.W. eds., Proceedings of the Ocean Drilling Program, Scientific Results, Volume 197: College Station, Texas, Ocean Drilling Program, p. 1–39, doi:10.2973/odp.proc.sr.197.001.2006.

Epp, D., 1984, Possible perturbations to hotspots trace and implications for the origin and structure of the Line Islands: Journal of Geophysical Research, v. 89, p. 11273–11286, doi:10.1029/JB089iB13p11273.

Escartin, J., Cannat, M., Pouliquen, G., Rabain, A., and Lin, J., 2001, Crustal thickness of V-shaped ridges south of the Azores: Interaction of the Mid-Atlantic Ridge (36°–39°N) and the Azores hot spot: Journal of Geophysical Research, v. 106, no. B10, p. 21719–21735, doi:10.1029/2001JB000224.

Fitton, J.G., 2007, The OIB paradox, *in* Foulger, G.R., and Jurdy, D.M., eds., Plates, Plumes and Planetary Processes: Geological Society of America Special Paper 430, p. 387–412, doi:10.1130/2007.2430(20).

Fitton, J.G., Saunders, A.D., Norry, M.J., Hardarson, B.S., and Taylor, R.N., 1997, Thermal and chemical structure of the Iceland plume: Earth and Planetary Science Letters, v. 153, p. 197–208, doi:10.1016/S0012-821X(97)00170-2.

Foulger, G.R., and Jurdy, D.M., eds., 2007, Plates, Plumes and Planetary Processes: Geological Society of America Special Paper 430, 998 p., doi:10.1130/978-0-8137-2430-0(2007)430.

Frey, F., Wise, W., Garcia, M.O., West, H., and Kwon, S.T., 1990, Evolution of Mauna Kea Volcano, Hawaii: Petrologic and geochemical constraints on post-shield volcanism: Journal of Geophysical Research, v. 95, p. 1271–1300, doi:10.1029/JB095iB02p01271.

Frey, F.A., Huang, S., Blichert-Toft, J., Regelous, M., and Boyet, M., 2005, Origin of depleted components in basalt related to the Hawaiian hot spot: Evidence from isotopic and incompatible element ratios: Geochemistry Geophysics Geosystems, v. 6, Q02L07, doi:10.1029/2004GC000757.

Funkhouser, J.G., Barnes, I.L., and Naughton, J.J., 1968, The determination of a series of ages of Hawaiian volcanoes by potassium-argon method: Pacific Science, v. 22, p. 369–372.

Garcia, M.O., Grooms, D.G., and Naughton, J.J., 1987, Petrology and geochronology of volcanic rocks from seamounts along and near the Hawaiian ridge: Implications for propagation rate of the ridge: Lithos, v. 20, p. 323–336, doi:10.1016/S0024-4937(87)80005-1.

Garcia, M.O., Caplan-Auerbach, J., De Carlo, E.H., Kurz, M.D., and Becker, N., 2006, Geology, geochemistry and earthquake history of Loihi seamount, Hawaii's youngest volcano: Chemie der Erde, v. 66, p. 81–108, doi:10.1016/j.chemer.2005.09.002.

Garcia, M.O., Haskins, E.H., and Stolper, E., 2007, Stratigraphy of the Hawaiian Scientific Drilling Project: Anatomy of a Hawaiian volcano: Geochemistry Geophysics Geosystems, v. 8, Q02G20, doi:10.1029/2006GC001379.

Garcia, M.O., Ito, G., Weis, D., Geist, D., Swinnard, L., Bianco, T., Flinders, A., Taylor, B., Appelgate, B., Blay, C., Hanano, D., Silva, I., Naumann, T., Maerschalk, C., Harpp, K., Christensen, B., Sciaroni, L, Tagami, T., and Yamasaki, S., 2008, Widespread secondary volcanism around the northern Hawaiian Islands: Eos (Transactions, American Geophysical Union), v. 89, p. 542–543, doi:10.1029/2008EO520002.

Garcia, M.O., Swinnard, L., Weis, D., Greene, A.R., Tagami, T., Sano, H., and Gandy, C.E., 2010, Geochemistry and geochronology of Kaua'i lavas over 4.5 Ma: Implications for the origin of rejuvenated volcanism and the

evolution of the Hawaiian plume: Journal of Petrology, v. 51, p. 1507–1540, doi:10.1093/petrology/egq027.

Greene, A.R., Garcia, M.O., Weis, D., Ito, G., Kuga, M., Robinson, J., and Yamasaki, S., 2010, Low-productivity Hawaiian volcanism between Kaua'i and O'ahu: Constraints on source composition and lithology: Geochemistry, Geophysics, Geosystems, v. 11, Q0AC08, doi:10.1029/2010GC003233.

Hanano, D., Weis, D., Scoates, J.S., Aciego, S., and DePaolo, D.J., 2010, Horizontal and vertical zoning of heterogeneities in the Hawaiian mantle plume from the geochemistry of consecutive post-shield volcano pairs: Kohala-Mahukona and Mauna Kea–Hualalai: Geochemistry Geophysics Geosystems, v. 11, Q01004, doi:10.1029/2009GC002782.

Hauri, E.H., 1996, Major-element variability in the Hawaiian mantle plume: Nature, v. 382, p. 415–419, doi:10.1038/382415a0.

Hieronymus, C.F., and Bercovici, D., 1999, Discrete alternating hotspot islands formed by interaction of magma transport and lithospheric flexure: Nature, v. 397, p. 604–607, doi:10.1038/17584.

Hofmann, A.W., 1988, Chemical differentiation of the Earth: The relationship between mantle, continental crust, and oceanic crust: Earth and Planetary Science Letters, v. 90, p. 297–314, doi:10.1016/0012-821X(88)90132-X.

Hofmann, A.W., 2003, Sampling mantle heterogeneity through oceanic basalts: Isotopes and trace elements, *in* Carlson, R.W., Holland, H.D., and Norry, M.I., eds., The Mantle and the Core: Treatise on Geochemistry Volume 2: London, Elsevier, p. 61–101.

Huang, S., Regelous, M., Thordarson, T., and Frey, F.A., 2005, Petrogenesis of lavas from Detroit Seamount: Geochemical differences between Emperor Chain and Hawaiian volcanoes: Geochemistry, Geophysics, Geosystems, v. 6, Q01L06, doi:10.1029/2004GC000756.

Huang, S., Hall, P.S., and Jackson, M.G., 2011, Geochemical zoning of volcanic chains associated with Pacific hotspots: Nature Geoscience, v. 4, p. 874–878, doi:10.1038/ngeo1263.

Ishizuka, O., Tani, K., Reagan, M.K., Kanayama, K., Umino, S., Harigane, Y., Sakamoto, I., Miyajima, Y., Yuasa, M., and Dunkley, D.J., 2011, The timescales of subduction initiation and subsequent evolution of an oceanic island arc: Earth and Planetary Science Letters, v. 306, p. 229–240, doi:10.1016/j.epsl.2011.04.006.

Ito, G., 2001, Reykjanes 'V'-shaped ridges originating from a pulsing and dehydrating mantle plume: Nature, v. 411, p. 681–684, doi:10.1038/35079561.

Jackson, E.D., Silver, E.A., and Dalrymple, G.B., 1972, Hawaiian-Emperor and its relation to Cenozoic circumpacific tectonics: Geological Society of America, v. 83, p. 601–618, doi:10.1130/0016-7606(1972)83[601:HCAIRT]2.0.CO;2.

Jackson, E.D., Koisumi, I., Dalrymple, G.A., Clague, D.A., Kirkpatrick, R.J., and Greene, H.G., 1980, Introduction and summary of results from DSDP Leg 55, The Hawaiian-Emperor hot-spot experiment, *in* Jackson, E.D., Koisumi, I., et al., Initial Reports of the Deep Sea Drilling Project, Volume 55: Washington, D.C., U.S. Government Printing Office, p. 5–31, doi:10.2973/dsdp.proc.55.101.1980.

Jackson, M.G., Weis, D., and Huang, S., 2012, Major element variations in Hawaiian shield lavas: Source features and perspectives from global ocean island basalt (OIB) systematics: Geochemistry Geophysics Geosystems, v. 13, Q09009, doi:10.1029/2012GC004268.

Jicha, B.R., Rhodes, J.M., Singer, B.S., and Garcia, M.O., 2012, The $^{40}Ar/^{39}Ar$ geochronology of submarine Mauna Loa volcano, Hawaii: Journal of Geophysical Research, v. 117, B09204, doi:10.1029/2012JB009373.

Jull, M., and McKenzie, D., 1996, The effect of deglaciation on mantle melting beneath Iceland: Journal of Geophysical Research, v. 101, p. 21815–21828, doi:10.1029/96JB01308.

Keller, R.A., Fisk, M.R., and White, W.M., 2000, Isotopic evidence for Late Cretaceous plume-ridge interaction at the Hawaiian hotspot: Nature, v. 405, p. 673–676, doi:10.1038/35015057.

Koppers, A.A., and Staudigel, H., 2005, Asynchronous bends in Pacific seamount trails: A case for extensional volcanism?: Science, v. 307, p. 904–907, doi:10.1126/science.1107260.

Koppers, A.A.P., Duncan, R. A., and Steinberger, B., 2004, Implications of a non-linear $^{40}Ar/^{39}Ar$ age progression along the Louisville seamount trail for models of fixed and moving hotspots: Geochemistry Geophysics Geosystems, v. 5, Q06L02, doi:10.1029/2003GC000671.

Koppers, A.A.P., Gowen, M.D., Colwell, L.E., Gee, J.S., Lonsdale, P.F., Mahoney, J.J., and Duncan, R.A., 2011, New $^{40}Ar/^{39}Ar$ age progression for the Louisville hot spot trail and implications for inter–hot spot motion: Geochemistry Geophysics Geosystems, v. 12, Q0AM02, doi:10.1029/2011GC003804.

Ladd, H.S., Tracy, J.I., and Gross, M.G., 1970, Deep drilling on Midway Atoll: U.S. Geological Survey Professional Paper 680-A, 22 p.

Lanphere, M.A., Dalrymple, G.B., and Clague, D.A., 1980, Rb-Sr systematics of basalts from the Hawaiian-Emperor volcanic chain, *in* Jackson, E.D., Koisumi, I., et al., Initial Reports of the Deep Sea Drilling Project, Volume 55: Washington, D.C., U.S. Government Printing Office, p. 695–706, doi:10.2973/dsdp.proc.55.131.1980.

Lee, C.-T.A., Luffi, P., Plank, T., Dalton, H., and Leeman, W.P., 2009, Constraints on the depths and temperatures of basaltic magma generation on Earth and other terrestrial planets using new thermobarometers for mafic magmas: Earth and Planetary Science Letters, v. 279, p. 20–33, doi:10.1016/j.epsl.2008.12.020.

Le Maître, R.W., ed., 2002, Igneous rocks. A Classification and Glossary of Terms. Recommendations of the International Union of Geological Sciences Subcommission on the Systematics of Igneous Rocks (second edition): Cambridge, UK, Cambridge University Press, 254 p.

Ludwig, K.R., Szabo, B.J., Moore, J.G., and Simmons, K.R., 1991, Crustal subsidence rate off Hawaii determined from $^{234}U/^{238}U$ ages of drowned coral reefs: Geology, v. 19, p. 171–174, doi:10.1130/0091-7613(1991)019<0171:CSROHD>2.3.CO;2.

Macdonald, G.A., and Katsura, T., 1964, Chemical composition of the Hawaiian lavas: Journal of Petrology, v. 5, p. 82–133, doi:10.1093/petrology/5.1.82.

Macdonald, G.A., Abbott, A.T., and Peterson, F.L., 1983, Volcanoes in the Sea: The Geology of Hawaii (second edition): Honolulu, University of Hawaii Press, 517 p.

Mark, R.K., and Moore, J.G., 1987, Slopes of the Hawaiian ridges: U.S. Geological Survey Professional Paper 1350, p. 101–107.

McDougall, I., 1971, Volcanic island chains and sea floor spreading: Nature Physical Science, v. 231, p. 141–144, doi:10.1038/physci231141a0.

Meffre, S., Falloon, T.J., Crawford, T.J., Hoernle, K., Hauff, F., Duncan, R.A., Bloomer, S.H., and Wright, D.J., 2012, Basalts erupted along the Tongan fore arc during subduction initiation: Evidence from geochronology of dredged rocks from the Tonga fore arc and trench: Geochemistry Geophysics Geosystems, v. 13, Q12003, doi:10.1029/2012GC004335.

Moore, J.G., 1965, Petrology of deep-sea basalt near Hawaii: American Journal of Science, v. 263, p. 40–52, doi:10.2475/ajs.263.1.40.

Moore, J.G., Clague, D.A., and Normark, W.R., 1982, Diverse basalt types from Loihi seamount, Hawaii: Geology, v. 10, p. 88–92, doi:10.1130/0091-7613(1982)10<88:DBTFLS>2.0.CO;2.

Morgan, W.J., 1971, Convection plumes in the lower mantle: Nature, v. 230, p. 42–43, doi:10.1038/230042a0.

Nobre Silva, I., Weis, D., Barling, J., and Scoates, J.S., 2009, Basalt leaching systematics and consequences for Pb isotopic compositions by MC-ICP-MS: Geochemistry Geophysics Geosystems, v. 10, Q08012, doi:10.1029/2009GC002537.

Nobre Silva, I.G., Weis, D., and Scoates, J.S., 2010, Effects of acid leaching on the Sr-Nd-Hf isotopic compositions of ocean island basalts: Geochemistry Geophysics Geosystems, v. 11, Q09011, doi:10.1029/2010GC003176.

O'Connor, J.M., Steinberger, B., Regelous, M., Koppers, A.A.P., Wijbrans, J.R., Haase, K.M., Stoffers, P., Jokat, W., and Garbe-Schönberg, D., 2013, Constraints on past plate and mantle motion from new ages for the Hawaiian-Emperor Seamount Chain: Geochemistry Geophysics Geosystems, v. 14, p. 4564–4584, doi:10.1002/ggge.20267.

Ozawa, A., Tagami, T., and Garcia, M.O., 2005, Unspiked K-Ar ages of Honolulu rejuvenated and Koolau shield volcanism on Oahu, Hawaii: Earth and Planetary Science Letters, v. 232, p. 1–11, doi:10.1016/j.epsl.2005.01.021.

Phipps Morgan, J., Morgan, W.J., and Price, E., 1995, Hotspot melting generates both hotspot volcanism and a hotspot swell?: Journal of Geophysical Research, v. 100, p. 8045–8062, doi:10.1029/94JB02887.

Quane, S., Garcia, M.O., Guillou, H., and Hulsebosch, T., 2000, Magmatic evolution of the East Rift Zone of Kilauea Volcano based on drill core from SOH 1: Journal of Volcanology and Geothermal Research, v. 102, p. 319–338, doi:10.1016/S0377-0273(00)00194-3.

Reagan, M.K., Ishizuka, O., Stern, R.J., Kelley, K.A., Ohara, Y., Blichert-Toft, J., Bloomer, S.H., Cash, J., Fryer, P., Hanan, B.B., Hickey-Vargas, R., Ishii, T., Kimura, J.-I., Peate, D.W., Rowe, M.C., and Woods, M., 2010, Fore-arc basalts and subduction initiation in the Izu-Bonin-Mariana system: Geochemistry Geophysics Geosystems, v. 11, Q03X12, doi:10.1029/2009GC002871.

Regelous, M., Hofmann, A.W., Abouchami, W., and Galer, S.J.G., 2003, Geochemistry of lavas from the Emperor Seamounts, and the geochemical

evolution of Hawaiian magmatism from 85 to 42 Ma: Journal of Petrology, v. 44, p. 113–140, doi:10.1093/petrology/44.1.113.

Rhodes, J.M., and Vollinger, M.J., 2004, Composition of basaltic lavas sampled by phase-2 of the Hawaii Scientific Drilling Project: Geochemical stratigraphy and magma types: Geochemistry Geophysics Geosystems, v. 5, Q03G13, doi:10.1029/2002GC000434.

Rhodes, J.M., Huang, S., Frey, F.A., Pringle, M., and Xu, G., 2012, Compositional diversity of Mauna Kea shield lavas recovered by the Hawaii Scientific Drilling Project: Inferences of source lithology, magma supply, and the role of multiple volcanoes: Geochemistry Geophysics Geosystems, v. 13, Q03014, doi:10.1029/2011GC003812.

Ribe, N.M., and Christensen, U.R., 1994, Three-dimensional modeling of plume-lithosphere interaction: Journal of Geophysical Research, v. 99, p. 669–682, doi:10.1029/93JB02386.

Ribe, N.M., and Christensen, U.R., 1999, The dynamical origin of Hawaiian volcanism: Earth and Planetary Science Letters, v. 171, p. 517–531, doi:10.1016/S0012-821X(99)00179-X.

Robinson, J.E., and Eakins, B.W., 2006, Calculated volumes of individual shield volcanoes at the young end of the Hawaiian ridge: Journal of Volcanology and Geothermal Research, v. 151, p. 309–317, doi:10.1016/j.jvolgeores.2005.07.033.

Sager, W.W., and Keating, B., 1984, Paleomagnetism of Line Islands seamounts: Evidence for Late Cretaceous and early Tertiary volcanism: Journal of Geophysical Research, v. 89, no. B13, p. 11135–11,151, doi:10.1029/JB089iB13p11135.

Schafer, J.T., Neal, C.R., and Regelous, M., 2005, Petrogenesis of Hawaiian post-shield lavas: Evidence from Nintoku Seamount, Emperor Seamount Chain: Geochemistry Geophysics Geosystems, v. 6, Q05L09, doi:10.1029/2004GC000875.

Sharp, W.D., and Clague, D., 2006, 50-Ma initiation if Hawaiian-Emperor bend records major change in Pacific plate motion: Science, v. 313, p. 1281–1284, doi:10.1126/science.1128489.

Sharp, W.D., and Renne, P.R., 2005, The $^{40}Ar/^{39}Ar$ and K/Ar dating of lavas, hyaloclastites and intrusions from the HSDP core hole: Geochemistry Geophysics Geosystems, v. 6, Q04G17, doi:10.1029/2004GC000846.

Sheth, H., 2007, Large igneous provinces (LIPs): Definition, recommended terminology, and a hierarchical classification: Earth-Science Reviews, v. 85, p. 117–124, doi:10.1016/j.earscirev.2007.07.005.

Sherrod, D.R., Sinton, J.M., Watkins, S.E., and Brunt, K.M., 2007, Geologic Map of the State of Hawai'i: U.S. Geological Survey Open-File Report 2007-1089, 83 p., scale 1:100,000 and 1:250,000.

Sinton, J., Grönvold, K., and Sæmundsson, K., 2005, Postglacial eruptive history of the Western Volcanic Zone, Iceland: Geochemistry Geophysics Geosystems, v. 6, Q12009, doi:10.1029/2005GC001021.

Sleep, N.H., 1990, Hotspots and mantle plumes: Some phenomenology: Journal of Geophysical Research, v. 95, p. 6715–6736, doi:10.1029/JB095iB05p06715.

Sleep, N.H., 1992, Hotspot volcanism and mantle plumes: Annual Review of Earth and Planetary Sciences, v. 20, p. 19–43, doi:10.1146/annurev.ea.20.050192.000315.

Smith, W.H.F., and Sandwell, D.T., 1997, Global seafloor topography from satellite altimetry and ship depth soundings: Science, v. 277, p. 1956–1962, doi:10.1126/science.277.5334.1956.

Sobolev, A.V., Hofmann, A.W., Kuzmin, D.V., Yaxley, G.M., Arndt, N.T., Chung, S.-L., Danyushevsky, L.V., Elliott, T., Frey, F.A., Garcia, M.O., Gurenko, A.A., Kamenetsky, V.S., Kerr, A.C., Krivolutskaya, N.A., Matvienkov, V.V., Nikogosian, I.K., Rocholl, A., Suschevskaya, N.M., and Teklay, M., 2007, Estimating the amount of recycled crust in sources of mantle derived melts: Science, v. 316, p. 412–417, doi:10.1126/science.1138113.

Spengler, S., and Garcia, M.O., 1988, Geochemical evolution of Hawi Formation lavas, Kohala Volcano, Hawaii: The hawaiite to trachyte transition: Contributions to Mineralogy and Petrology, v. 99, p. 90–104, doi:10.1007/BF00399369.

Tanaka, R., Makishima, A., and Nakamura, E., 2008, Hawaiian double volcanic chain triggered by an episodic involvement of recycled material: Constraints from temporal Sr-Nd-Hf-Pb isotopic trend of the Loa-type volcanoes: Earth and Planetary Science Letters, v. 265, p. 450–465, doi:10.1016/j.epsl.2007.10.035.

Tarduno, J., Duncan, R.A., Scholl, D.W., Cottrell, R.D., Steinberger, B., Thordarson, T., Kerr, B.C., Neal, C.R., Frey, F.A., Torii, M., and Carvallo, C., 2003, The Emperor Seamounts: Southward motion of the Hawaiian hotspot plume in Earth's mantle: Science, v. 301, p. 1064–1069, doi:10.1126/science.1086442.

Tarduno, J., Bunge, H.P., Sleep, N., and Hansen, U., 2009, The bent Hawaiian-Emperor hotspot track: Inheriting the mantle wind: Science, v. 324, p. 50–53, doi:10.1126/science.1161256.

Tatsumoto, M., 1978, Isotopic composition of lead in oceanic basalt and its implication to mantle evolution: Earth and Planetary Science Letters, v. 38, p. 63–87, doi:10.1016/0012-821X(78)90126-7.

Van Ark, E., and Lin, J., 2004, Time variation in igneous volume flux of the Hawaii-Emperor hot spot seamount chain: Journal of Geophysical Research, v. 109, B11401, doi:10.1029/2003JB002949.

Vanderkluysen, L., Mahoney, J.J., Koppers, A.A.P., Beier, C., Regelous, M., Gee, J., and Lonsdale, P.F., 2014, Louisville Seamount Chain: Petrogenetic processes, and geochemical evolution of the mantle source: Geochemistry Geophysics Geosystems, v. 15, p. 2380–2400, doi:10.1002/2014GC005288.

Vidal, V., and Bonneville, A., 2004, Variations of the Hawaiian hot spot activity revealed by variations in the magma production rate: Journal of Geophysical Research, v. 109, B03104, doi:10.1029/2003JB002559.

Vogt, P.R., 1972, Evidence for global synchronism in mantle plume convection, and possible significance for geology: Nature, v. 240, no. 5380, p. 338–342, doi:10.1038/240338a0.

Von Herzen, R.P., Cordery, M.J., Detrick, R.S., and Fang, C., 1989, Heat flow and thermal origin of hot spot swells: The Hawaiian Swell revisited: Journal of Geophysical Research, v. 94, p. 13,783–13,799, doi:10.1029/JB094iB10p13783.

Walker, G.P.L., 1990, Geology and volcanology of the Hawaiian Islands: Pacific Science, v. 44, p. 315–347.

Weis, D., Kieffer, B., Maerschalk, C., Barling, J., de Jong, J., Williams, G.A., Hanano, D., Pretorius, W., Mattielli, N., Scoates, J.S., Goolaerts, A., Friedman, R.M., and Mahoney, J.B., 2006, High-precision isotopic characterization of USGS reference materials by TIMS and MC-ICP-MS: Geochemistry Geophysics Geosystems, v. 7, Q08006, doi:10.1029/2006GC001283.

Weis, D., Garcia, M.O., Rhodes, J.M., Jellinek, M., and Scoates, J.S., 2011, Role of the deep mantle in generating the compositional asymmetry of the Hawaiian mantle plume: Nature Geoscience, v. 4, p. 831–838, doi:10.1038/ngeo1328.

Wessel, P., and Kroenke, L.W., 2009, Observations of geometry and ages constrain relative motion of Hawaii and Louisville plumes: Earth and Planetary Science Letters, v. 284, p. 467–472, doi:10.1016/j.epsl.2009.05.012.

Wessel, P., and Smith, W.H.F., 1991, Free software helps map and display data: Eos (Transactions, American Geophysical Union), v. 72, p. 441–446, doi:10.1029/90EO00319.

Wessel, P., Harada, Y., and Kroenke, L.W., 2006, Toward a self-consistent, high-resolution absolute plate motion model for the Pacific: Geochemistry Geophysics Geosystems, v. 7, Q03L12, doi:10.1029/2005GC001000.

White, R.S., 1993, Melt production rates in mantle plumes: Royal Society of London Philosophical Transactions, ser. A, v. 342, no. 1663, p. 137–153, doi:10.1098/rsta.1993.0010.

Wilson, J.T., 1963, Evidence from islands on the spreading of the ocean floor: Canadian Journal of Physics, v. 41, p. 863–870, doi:10.1139/p63-094.

Winchell, H., 1947, Honolulu Series, Oahu, Hawaii: Geological Society of America Bulletin, v. 58, p. 1–48, doi:10.1130/0016-7606(1947)58[1:HSOH]2.0.CO;2.

Wolfe, C.J., Solomon, S.C., Laske, G., Collins, J.A., Detrick, R.S., Orcutt, J.A., Bercovici, D., and Hauri, E.H., 2011, Mantle P-wave velocity structure beneath the Hawaiian hotspot: Earth and Planetary Science Letters, v. 303, p. 267–280, doi:10.1016/j.epsl.2011.01.004.

Wolfe, E.W., Wise, W.S., and Dalrymple, G.B., 1997, The geology and petrology of Mauna Kea volcano: U.S. Geological Survey Professional Paper 129, 129 p.

Wright, T.L., 1971, Chemistry of Kilauea and Mauna Loa lava in space and time: U.S. Geological Survey Professional Paper 735, 40 p.

Zindler, A., Staudigel, H., and Batiza, R., 1984, Isotope and trace element geochemistry of young Pacific seamounts; implications for the scale of upper mantle heterogeneity: Earth and Planetary Science Letters, v. 70, p. 175–195, doi:10.1016/0012-821X(84)90004-9.

Manuscript Accepted by the Society 10 November 2014
Manuscript Published Online 9 April 2015

Geological Society of America Special Papers

Petrology, geochemistry, and ages of lavas from Northwest Hawaiian Ridge volcanoes

Michael O. Garcia, John R. Smith, Jonathan P. Tree, et al.

Geological Society of America Special Papers 2015;511; 1-25 , originally published onlineFebruary 12, 2015
doi:10.1130/2015.2511(01)

Notes